



CORSIKA 8

Contributions to the 37th International Cosmic Ray Conference in Berlin Germany (ICRC 2021)

The CORSIKA 8 Collaboration

Full Authors List:

Jean-Marco Alameddine^b, Johannes Albrecht^b, Jaime Alvarez-Muniz^r, Antonio Augusto Alves Jr^d, Luisa Arrabito^a, Dominik Baack^b, Konrad Bernlöhner^c, Marcus Bleicher^o, Johan Bregeon^s, Mathieu Carrere^a, Hans Dembinski^b, Hannah Elfnerⁱ, Dominik Elsässer^b, Ralph Engel^d, Hu Fan^p, Anatoli Fedynitch^j, Dieter Heck^d, Tim Huege^{d,e}, Karl-Heinz Kampert^k, Nikolaos Karastathis^d, Lukas Nellen^f, Maximilian Nöthe^b, David Parello^t, Tanguy Pierog^d, Maria Pokrandt^d, Anton Poctarev^d, Remy Prechelt^l, Maximilian Reininghaus^{d,m}, Wolfgang Rhode^b, Felix Riehn^{h,r}, Maximilian Sackel^b, Alexander Sandrock^u, Pranav Sampathkumar^d, Michael Schmelling^c, André Schmidt^d, Günter Siglⁿ, Jan Soedingrekso^b, Bernhard Spaan^b, Donglian Xu^q, Juan Ammerman-Yebra^r, Enrique Zas^r and Ralf Ulrich^d



^aLaboratoire Univers et Particules, Université de Montpellier 2, Montpellier, France, ^bExperimentelle Physik 5, TU Dortmund, Dortmund, Germany, ^cMax Planck Institute for Nuclear Physics, Heidelberg, Germany, ^dInstitute for Astroparticle Physics, Karlsruhe Institute of Technology, Karlsruhe, Germany, ^eAstrophysical Institute, Vrije Universiteit Brussel, Brussels, Belgium ^fNational Autonomous University of Mexico, Mexico City, Mexico, ^gInstituto de Tecnologías en Detección y Astropartículas, Buenos Aires, Argentina, ^hLaboratory of Instrumentation and Experimental Particles, Lisbon, Portugal, ⁱHelmholtzzentrum für Schwerionenforschung, Darmstadt, Germany, ^jInstitute for Cosmic Ray Research, The University of Tokyo, Tokyo, Japan, ^kLehrstuhl für Astroteilchenphysik, Bergische Universität Wuppertal, Wuppertal, Germany, ^lDepartment of Physics & Astronomy, University of Hawai'i at Manoa, Honolulu, USA, ^mInstituto de Tecnologías en Detección y Astropartículas, Buenos Aires, Argentina, ⁿII Institut für Theoretische Physik, Universität Hamburg, Hamburg, Germany, ^oJohann-Wolfgang-Goethe-Universität, Frankfurt am Main, Germany, ^pPeking University, Beijing, China, ^qTsung-Dao Lee Institute, Shanghai, China, ^rInstituto Galego de Física de Altas Enerxías, Universidade de Santiago de Compostela, Santiago de Compostela, Spain, ^sLaboratoire de Physique Subatomique et de Cosmologie, Grenoble, France, ^tLIRMM, Univ Montpellier, CNRS, Montpellier, France, ^uNational Research Nuclear University, Moscow Engineering Physics Institute, Moscow, Russia.

Contributions

1) Status of the novel CORSIKA 8 air shower simulation framework: <i>A. Augusto Alves Jr.,</i> PoS (ICRC2021) 284	2
2) Simulations of radio emission from air showers with CORSIKA 8: <i>Nikolaos Karastathis,</i> PoS (ICRC2021) 427	11
3) Electromagnetic Shower Simulation for CORSIKA 8: <i>Jean-Marco Alameddine,</i> PoS (ICRC2021) 428	20
4) Air shower genealogy for muon production: <i>Maximilian Reininghaus,</i> PoS (ICRC2021) 463	28
5) Hadron cascades in CORSIKA 8: <i>Ralf Ulrich,</i> PoS (ICRC2021) 474	36
6) GPU accelerated optical light propagation in CORSIKA 8: <i>Dominik Baack,</i> PoS (ICRC2021) 705	44

Status of the novel CORSIKA 8 air shower simulation framework

A. Augusto Alves Jr^{a,*} on behalf of the CORSIKA 8 Collaboration

(a complete list of authors can be found at the end of the proceedings)

^a*Institut für Astroteilchenphysik - Karlsruher Institut für Technologie
Karlsruhe, Germany*

E-mail: augusto.alvesjunior@kit.edu

The CORSIKA 8 project is an international collaboration of scientists working together to implement a modern, flexible, robust and efficient framework for the simulation of ultra-high energy secondary particle cascades in matter. While the main application is for simulating cosmic ray air showers, the project aim to useful to other problems in astro(particle), particle and nuclear physics. Besides a comprehensive and state-of-the-art collection of physics models and algorithms relevant for the field, interfaces to deployment modern multicore processors and hardware accelerators (e.g. GPU) are also planned. This contribution presents the status and roadmap of the CORSIKA 8 project.

*37th International Cosmic Ray Conference (ICRC 2021)
July 12th – 23rd, 2021
Online – Berlin, Germany*

*Presenter

1. Introduction

The legacy CORSIKA air shower simulation program[1] has been the de facto common reference frame for a vast class of measurements and studies in astroparticle physics for almost 30 years [2], making it possible to perform accurate comparative, incremental and progressive research in the field.

The CORSIKA 8 project[3] is basically the follow-up on this approach and aims to port and to implement it into a modern computing fashion. The effort is fundamentally community-driven and bundles modern concepts for computing with the goal for the most comprehensive and flexible physics description for the simulation of particle cascades. It will bring novel modularity to enable optimal and fine-tuned modeling as well as future developments. Among other planned features, it will be possible to better relate the importance of model parameter uncertainties on observables of interest and to incorporate improvements in physics related algorithms, where it is applicable. Concomitantly, a significant effort is being devoted to deploy concepts and techniques connected with modern high-performance computing through robust and user-friendly interfaces. For example, the need to balance high performance goals, with portability and modularity lead to the adoption of C++ as the basic language of the framework.

In these proceedings, the key features of CORSIKA 8, as well as some very basic comparison of simulation results, are discussed.

2. Scientific context and open problems

The understanding of the formation of secondary particle cascades due to the interaction of high energy particles with the matter is a central problem in astroparticle physics. Indeed, these phenomena occur in many astrophysically relevant contexts, producing gamma-ray and neutrino emissions. When happening in Earth's atmosphere, the penetration of high energy cosmic-rays produces extensive air shower cascades (EAS), which are then observed by experiments.

The precise interpretation of the corresponding experimental data in terms of fundamental properties of the matter and the primary cosmic ray particles is crucial for understanding many aspects of the nature of the physics phenomena in the surround universe. As the involved energies increase, the more relevant are the opportunities for a more precise measurement of the primary composition of cosmic rays and also for understanding how such particles interact.

The precise description of EAS is a very challenging endeavor. Hadron collisions must be described with good quality from hundreds of TeV down to GeV, at center-of-mass energy. This, most importantly, includes the relatively poorly known forward phase space, which requires dedicated input from experiments at accelerators. Cascades develop in air, which is a mixture of light elements, making the modelling of nuclear effects very important. Electromagnetic interactions must consider the density-dependent high-energy Landau-Pomeranchuk-Migdal (LPM) effect [4–6] which suppresses cross-sections at high energies as well as density-corrections at low energies.

Astroparticle physics observatories depend on the modelling of EAS for their design, operation and also for their data analyses. This is most obvious for indirect cosmic ray experiments, regardless if they measure particles at ground, fluorescence light, Cherenkov light, radio emission, or something else (e.g. [7]). But also neutrino observatories require a very precise understanding of their

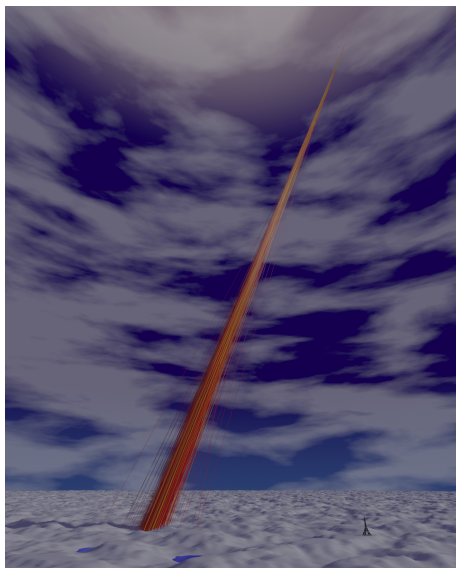


Figure 1: Example of a simulated proton shower at $E_0 = 10^7 \text{ GeV}$ with CORSIKA 8 representing the propagation and interaction of hadrons and muons in earth magnetic field. Only particles above 50 GeV are represented. Red are muons, yellow are hadrons.

atmospheric backgrounds, which are immense and extremely difficult to simulate. Finally, also the PeV gamma ray observatories need simulations for signal and background studies, sometimes even in a time-dependent and per-source setting[8].

Thus, basically all emission produced in EAS are used by experiments. CORSIKA 8 is the tool linking microscopic models to the final experimental observables. One of the big challenges is the better understanding of how uncertainties in input models affect observables.

In fig. 1 the 3D output of one EAS simulation performed with CORSIKA 8 is shown.

3. Design overview and infrastructure

As framework, CORSIKA 8 is designed to provide most, if not all, the infrastructure necessary to write concrete physics applications. The central loop involves a stack used for temporary storage of particles, a geometric transport routines and a list of processes that can lead to secondary-particle production or absorption. In terms of interpretation, the main goals driving the development summarized below.

- **Modularity:** It is a fundamental requirement that all algorithms and physics models are interfaced in a transparent, simple and modular way. Each physics process is provided as a *module*, with clear scope and having all necessary assumptions and parameters configurable. Among others conveniences, this design eases the implementation of new models, to extend or replace the delivered functionality. The different types of modules describing the physics of cascades are represented by C++ class templates: `ContinuousProcess`, `InteractionProcess`, `DecayProcess`, `SecondariesProcess`, `StackProcess`, `BoundaryCrossingProcess` [9].

- **Completeness:** In order to perform accurate studies on systematic effects and generate comprehensive comparisons, CORSIKA 8 aims to provide interfaces for the most, if not all, approaches available in the literature to deal with a given problem.
- **Robustness:** In order to enable CORSIKA 8 to run over decades, a set of design choices has been made to ensure long-term stability. For example, the usage of plain old data (POD) C++ types is avoided in favor of statically typed constructs, e.g. `ContinuousProcessIndex` instead of just `int`, particle codes are enumerated like in `Code code=Electron;`. Statically typed units are used to express physics properties, like in `HEPEnergyType E0 = 10_GeV;` [10]. Such choices allow the compiler to perform extensive checks on the correctness of expressions, avoiding the most common mistakes.
- **Performance:** Specific attention is devoted to provide efficient implementations for core algorithms and modules. In particular, extensive support for modern multithread architectures, like multicore CPUs and GPUs is planned.

The CORSIKA 8 framework deploy a set of innovative and state-of-the-art computing techniques and programming patterns to deal with pseudorandom number generation, track the history of secondary cascades, output and storage data. These and other implementation details are discussed in [11–13].

4. Physics modules

In terms of physics related features, CORSIKA 8 is not yet complete. Currently, available event generators for hadron collisions are SIBYLL2.3d [14], QGSJetII.04 [15], PYTHIA 8 [16] and UrQMD [17]. The latter is used at "low" energies (typically below around 100 GeV), while the former two can go up to the highest energies. The electromagnetic interactions and continuous/radiative energy losses of leptons are simulated with PROPOSAL [18–20]. Decays are currently delegated to PYTHIA 8 or SIBYLL. Charged particles moving in magnetic fields are tracked using a leap-frog algorithm. The region of interest, containing an environment potentially filled with different media is described using a custom geometry set of functionality, allowing the definition of different materials on large scales, to model situations like showers in the atmosphere which penetrate and get detected inside an ice shield at the South Pole. Thanks to the clear and simple interfaces, further physics modules can be easily added as it become available.

5. Examples and preliminary results,

The functionality implemented in CORSIKA 8, albeit incomplete, allows the usage of the framework to perform a range of useful calculations, such as validation studies. It also provides insights for new types of research that maybe were not feasible before.

More specifically, the available physics modules for the hadronic and muonic shower components [13, 21] can be used for performing cross-validation with other air shower simulation codes, including legacy CORSIKA versions. For example, the fig. 2a shows the comparison of the energy spectra of secondary particles reaching the ground as obtained from simulations with CORSIKA 8,

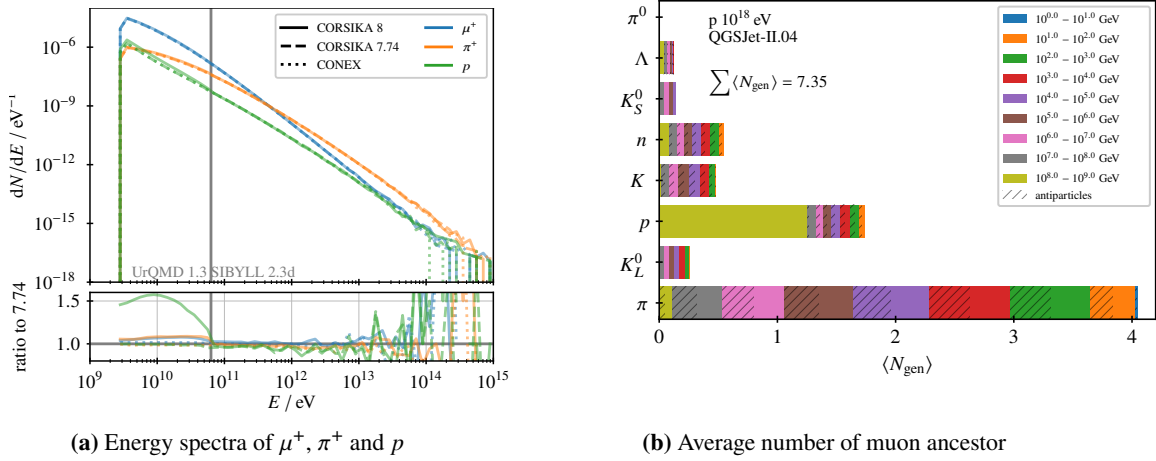


Figure 2: On the left, the energy spectra of μ^+ , π^+ and p of 1×10^{17} eV vertical proton shower, averaged over 400 events. On the right, the average number of muon ancestor projectile generations by particle species and energy.

CORSIKA 7.74 and CONEX [22] using the same parameters and interaction models in all three codes (vertical proton primary of 10^{17} eV, SIBYLL 2.3d and UrQMD 1.3 for hadronic interactions above and below 63.1 GeV, respectively). A good agreement is observed in the high energy regime. The low energy region exhibits some significant differences in the spectra of nucleons, which are attribute to differences in the interfaces to the event generator. The impact on the muon spectra, however, is small. First detailed results of such comparisons have been published elsewhere [23] and further studies are ongoing.

The fig. 2b represents a first application using the cascade history tracking, recently implemented and lengthily described in [12, 13], the ancestry of projectiles that finally lead to a muon on ground[12]. At energies between the primary energy (10^{18} eV) and down to about a decade less, nucleon interactions dominate, with only a small fraction being antinucleons. Especially the impact of the primary proton is visible as it is the unique particle in the "zeroth generation" of all shower particles and therefore contributes 1 to $\langle N_{\text{gen}} \rangle$ in the highest energy bin. At lower energies ($\lesssim 10^{17}$ eV), pion interaction are the main driver of the hadronic cascade and each decade in energy contributes roughly equally to the number of generations until around several 10 GeV they decay into muons and almost no pion interacts again below 10 GeV.

Concomitantly, dedicated modules deploying efficient computing techniques, like GPU based acceleration and vectorization, are under development for calculation of Cherenkov and radio emissions[24–27]. The fig. 3b shows an example of Cherenkov light emission simulation in GPU, calculated at ground level for a shower produced by a 1TeV gamma ray. The fig. 3a represents the pulse produced by radio using both algorithms CoREAS and ZHS running at CORSIKA 8, by a vertical electron shower of 100 TeV, on a layered atmosphere with a uniform refractive index of 1.000327 and a geomagnetic field $50\mu\text{T}$ in the x-direction. The antenna is placed at 200m from the shower core.

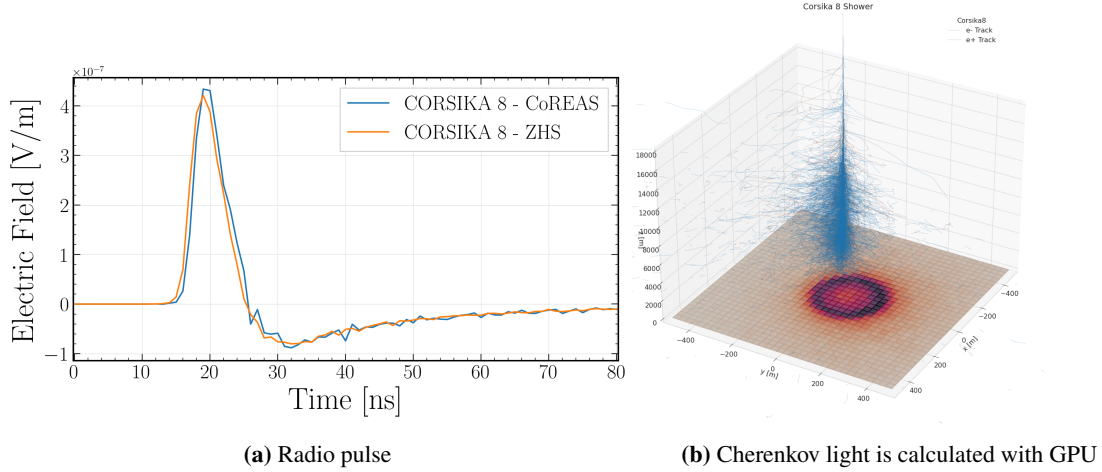


Figure 3: On the left, a pulse produced by radio using both algorithms CoREAS and ZHS, by a vertical electron shower of 100 TeV. On the right, the Cherenkov light at ground level simulated in CORSIKA 8 using GPU.

6. Summary and roadmap

CORSIKA 8 framework, a novel high-performance computing platform for simulations of secondary particle cascades in astroparticle physics has been described. The framework is written in C++17 and planned for supporting modern hardware architectures like multicore CPU and accelerators like GPUs and FPGAs, for running suited sub-problems with increased performance.

A first pre-release version is available for tests, validation and development [28]. This includes physics models, geometry, environment/media, output and configuration. Such a version should be used by the community for extensive tests, in order to provide the feedback needed for refinements and corrections, leading to a first full physics production release. It is foreseen that the setup as an open-source community project will support the goal for continued development over a very extended period of time.

Acknowledgments

The authors acknowledge support by the High Performance and Cloud Computing Group at the Zentrum für Datenverarbeitung of the University of Tübingen, the state of Baden-Württemberg through bwHPC and the German Research Foundation (DFG) through grant no. INST 37/935-1 FUGG.

References

- [1] D. Heck, J. Knapp, J.N. Capdevielle, G. Schatz and T. Thouw, *CORSIKA: A Monte Carlo code to simulate extensive air showers*, Tech. Rep. FZKA-6019, Forschungszentrum Karlsruhe (1998), DOI.
- [2] H.J. Gils, D. Heck, J. Oehlschlaeger, G. Schatz, T. Thouw and A. Merkel, A MULTITRANSPUTER SYSTEM FOR PARALLEL MONTE CARLO SIMULATIONS OF EXTENSIVE AIR SHOWERS, *Comput. Phys. Commun.* **56** (1989) 105.

- [3] R. Engel, D. Heck, T. Huege, T. Pierog, M. Reininghaus, F. Riehn et al., *Towards a Next Generation of CORSIKA: A Framework for the Simulation of Particle Cascades in Astroparticle Physics*, *Comput. Softw. Big Sci.* **3** (2019) 2 [1808.08226].
- [4] A.B. Migdal, *Bremsstrahlung and pair production in condensed media at high-energies*, *Phys. Rev.* **103** (1956) 1811.
- [5] L.D. Landau and I. Pomeranchuk, *Electron cascade process at very high-energies*, *Dokl. Akad. Nauk Ser. Fiz.* **92** (1953) 735.
- [6] L.D. Landau and I. Pomeranchuk, *Limits of applicability of the theory of bremsstrahlung electrons and pair production at high-energies*, *Dokl. Akad. Nauk Ser. Fiz.* **92** (1953) 535.
- [7] R. Smida et al., *Observation of microwave emission from extensive air showers with CROME*, *EPJ Web Conf.* **53** (2013) 08010.
- [8] E. Santos for AUGER Collaboration, *Monte Carlo simulations for the Pierre Auger Observatory using the VO Auger grid resources*, in *Proceedings of 37th International Cosmic Ray Conference (ICRC 2021)* [29], <https://pos.sissa.it/395/232/>.
- [9] M. Reininghaus and R. Ulrich, *CORSIKA 8 – Towards a modern framework for the simulation of extensive air showers*, *EPJ Web Conf.* **210** (2019) 02011 [1902.02822].
- [10] CORSIKA 8 collaboration, *Technical Foundations of CORSIKA 8: New Concepts for Scientific Computing*, *PoS ICRC2019* (2020) 236.
- [11] A.A. Alves Junior, A. Pochtarev and R. Ulrich, *Counter-based pseudorandom number generators for CORSIKA 8: A multi-thread friendly approach*, in *Proceedings of 25th International Conference on Computing in High Energy and Nuclear Physics (CHEP 2021)* [30], <https://indico.cern.ch/event/948465/contributions/4324156/>.
- [12] R. Ulrich, A.A. Alves Junior, M. Reininghaus, R. Prechelt and A. Schmidt, *CORSIKA 8 - A novel high-performance computing tool for particle cascade Monte Carlo simulations*, in *Proceedings of 25th International Conference on Computing in High Energy and Nuclear Physics (CHEP 2021)* [30], <https://indico.cern.ch/event/948465/contributions/4324165/>.
- [13] M. Reininghaus for CORSIKA 8 Collaboration, *Air shower genealogy for muon production*, in *Proceedings of 37th International Cosmic Ray Conference (ICRC 2021)* [29], <https://pos.sissa.it/395/463/>.
- [14] F. Riehn, R. Engel, A. Fedynitch, T.K. Gaisser and T. Stanev, *Hadronic interaction model Sibyll 2.3d and extensive air showers*, *Phys. Rev. D* **102** (2020) 063002 [1912.03300].
- [15] S. Ostapchenko, *Monte Carlo treatment of hadronic interactions in enhanced Pomeron scheme: I. QGSJET-II model*, *Phys. Rev. D* **83** (2011) 014018 [1010.1869].
- [16] T. Sjöstrand, S. Ask, J.R. Christiansen, R. Corke, N. Desai, P. Ilten et al., *An introduction to PYTHIA 8.2*, *Comput. Phys. Commun.* **191** (2015) 159 [1410.3012].

- [17] M. Bleicher et al., *Relativistic hadron hadron collisions in the ultrarelativistic quantum molecular dynamics model*, *J. Phys. G* **25** (1999) 1859 [hep-ph/9909407].
- [18] J.-M. Alameddine, J. Soedingrekso, A. Sandrock, M. Sackel and W. Rhode, *PROPOSAL: A library to propagate leptons and high energy photons*, *J. Phys. Conf. Ser.* **1690** (2020) 012021.
- [19] M. Dunsch, J. Soedingrekso, A. Sandrock, M. Meier, T. Menne and W. Rhode, *Recent Improvements for the Lepton Propagator PROPOSAL*, *Comput. Phys. Commun.* **242** (2019) 132 [1809.07740].
- [20] J.H. Koehne, K. Frantzen, M. Schmitz, T. Fuchs, W. Rhode, D. Chirkin et al., *PROPOSAL: A tool for propagation of charged leptons*, *Comput. Phys. Commun.* **184** (2013) 2070.
- [21] R. Ulrich for CORSIKA 8 Collaboration, *Hadron cascades in CORSIKA 8*, in *Proceedings of 37th International Cosmic Ray Conference (ICRC 2021)* [29], <https://pos.sissa.it/395/474/>.
- [22] T. Bergmann, R. Engel, D. Heck, N.N. Kalmykov, S. Ostapchenko, T. Pierog et al., *One-dimensional Hybrid Approach to Extensive Air Shower Simulation*, *Astropart. Phys.* **26** (2007) 420 [astro-ph/0606564].
- [23] CORSIKA 8 collaboration, *First results of the CORSIKA 8 air shower simulation framework*, *PoS ICRC2019* (2020) 399.
- [24] N. Karastathis for CORSIKA 8 Collaboration, *Simulations of radio emission from air showers with CORSIKA 8*, in *Proceedings of 37th International Cosmic Ray Conference (ICRC 2021)* [29], <https://pos.sissa.it/395/427/>.
- [25] J.M. Alameddine for CORSIKA 8 Collaboration, *Electromagnetic Shower Simulation for CORSIKA 8*, in *Proceedings of 37th International Cosmic Ray Conference (ICRC 2021)* [29], <https://pos.sissa.it/395/428/>.
- [26] D. Baack for CORSIKA 8 Collaboration, *GPU Accelerated optical light propagation in CORSIKA8*, in *Proceedings of 37th International Cosmic Ray Conference (ICRC 2021)* [29], <https://pos.sissa.it/395/705/>.
- [27] L. Arrabito, D. Parello, J. Bregeon, P. Langlois and G. Vasileiadis, *A C++ Cherenkov photons simulation in CORSIKA 8*, in *Proceedings of 25th International Conference on Computing in High Energy and Nuclear Physics (CHEP 2021)* [30], <https://indico.cern.ch/event/948465/contributions/4324127/>.
- [28] <https://gitlab.ikp.kit.edu/AirShowerPhysics/corsika>.
- [29] *Proceedings of 37th International Cosmic Ray Conference (ICRC 2021)*, PoS ICRC2021, To appear.
- [30] *Proceedings of 25th International Conference on Computing in High Energy and Nuclear Physics (CHEP 2021)*, EPJ Web of Conf., To appear.

Simulations of radio emission from air showers with CORSIKA 8

Nikolaos Karastathis,^{a,*} Remy Prechelt,^b Tim Huege^{a,d} and Juan Ammerman-Yebra^c
on behalf of the CORSIKA 8 Collaboration

(a complete list of authors can be found at the end of the proceedings)

^a*Institute for Astroparticle Physics (IAP), Karlsruhe Institute of Technology, Karlsruhe, Germany*

^b*Department of Physics and Astronomy, University of Hawai'i Mānoa, Honolulu, USA*

^c*Instituto Galego de Física de Altas Enerxías (IGFAE), Universidade de Santiago de Compostela, 15782 Santiago de Compostela, Spain*

^d*Astrophysical Institute, Vrije Universiteit Brussel, Brussels, Belgium*

E-mail: nikolaos.karastathis@kit.edu

CORSIKA 8 is a new framework for air shower simulations implemented in modern C++17, based on past experience with existing codes like CORSIKA 7. The flexibility of this framework allows for the inclusion of radio-emission calculations as an integral part of the program. Our design makes radio simulations general and gives the user the freedom to choose between different formalisms, such as the “Endpoints” and “ZHS” formalisms. In addition, it takes advantage of the flexibility of the CORSIKA 8 environment and geometry design, allowing future updates to more complex scenarios such as showers crossing from air into dense media. We present first results, along with comparisons with other simulation programs like CoREAS in CORSIKA 7 and ZHAireS. In the future, based on our design, the opportunity arises for radio simulations to achieve a significant boost in performance by deploying parallel computing techniques, in particular employing GPUs, and hence, perform more sophisticated radio-emission studies.

37th International Cosmic Ray Conference (ICRC 2021)
July 12th – 23rd, 2021
Online – Berlin, Germany

*Presenter

1. Introduction

Radio detection of extensive air showers has matured and become a technique competitive with “classical” particle and fluorescence detection over the past 20 years [1]. Due to the complexity of extensive air showers (EAS), detailed particle-level simulations of the radio emission of EAS are needed to analyze experimental data and reconstruct the properties of the primary particle. The two standard simulation tools used for simulations of the radio emission from showers are CoREAS [2] (implemented in CORSIKA 7 [3]) and ZHAireS [8]. These tools implement two different formalisms for calculating the radio emission from the particle tracks in the extensive air shower, namely the “Endpoint” formalism [4, 5] and the “ZHS” [7] formalism, respectively. However, these implementations inherit the limitations of their underlying shower codes and are not able to simulate the diverse array of current and future experiments (see section 1.1). Furthermore, as proposed next-generation experiments are growing significantly in size and channel-count, the computational cost of calculating the radio emission (especially for ultra high-energy showers) becomes intractable. To address these limitations, we have implemented the first radio emission module for the CORSIKA 8 (C8) shower simulation framework that is designed to be highly configurable and user-extensible to directly address the limitations of the current simulation tools and support the next generation of radio experiments.

1.1 Limitations of existing air shower simulation codes

The current generation of air shower simulation tools, CORSIKA 7 (C7) and ZHAireS, have several fundamental limitations that prevent their application to current and next-generation radio cosmic-ray and neutrino experiments. In particular,

Fixed down-going event geometry Both ZHAireS and C7 assume a flat or curvilinear approximation to the Earth and assume that all extensive air showers propagate downwards to the ground.¹ Many funded and proposed experiments are sensitive to upwards-going air showers induced by τ -leptons stratospheric cosmic-rays that never intersect the ground, or cosmic rays that are seen in *reflection* off the Earth’s surface, none of which can be simulated with the established simulation tools. Furthermore, the approximate treatment of the curvature of the Earth in existing tools can introduce significant errors for highly-inclined downgoing-showers.

Straight-ray approximation Both existing codes assume that the radio emission propagates in a straight line from the emitting particle track to the receiver (i.e. the antenna), ignoring the refraction (or diffraction) of the radio emission as it propagates through the (potentially) changing refractivity of propagation medium. For highly-inclined or upgoing shower geometries, or for showers in media with strong refractivity gradients (i.e. polar ice), the ray curvature can be significant.

Fixed shower media The existing tools typically also only work with pre-programmed atmosphere models and are not easily configurable for alternate media which is a major limitation for the current and proposed experiments that need to simulate cosmic-ray or neutrino-induced showers in ice, the lunar regolith and even first air and then a dense medium.

¹This statement applies to the official release versions - modified versions do exist but are available upon request.

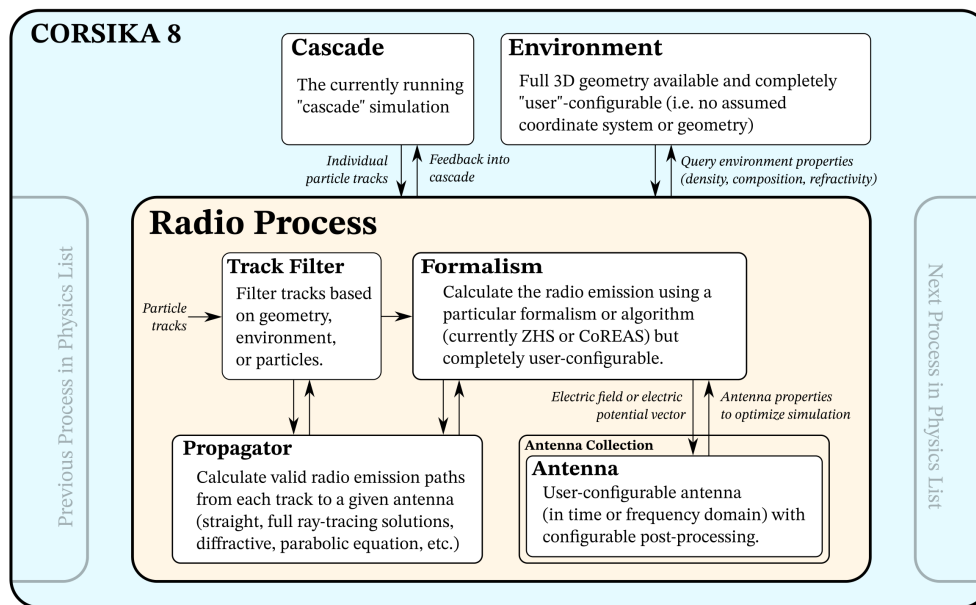


Figure 1: A schematic diagram of the radio process currently implemented in C8 and how it integrates with the C8 framework.

The design and implementation of the radio module in C8 has been tailored to address all of these limitations and provide a completely configurable and programmable platform to support the current and next generation of terrestrial and extra-terrestrial radio cosmic-ray and neutrino experiments.

2. Architecture of Radio Emission Calculation in CORSIKA 8

The radio *module* builds on C8’s highly modular and extensible design to support the next generation of air shower experiments. The top-level architecture of the radio *process* is shown in Figure 1. Each component shown in Fig. 1 can be independently swapped out with CORSIKA-provided or user-provided C++ code providing that they implement the required interfaces. The four primary configurable components are:

Filter The *Filter* is responsible for deciding which particles and tracks received from C8 should be forwarded to the radio emission calculation. This can be used to optimize the performance of the radio calculation by only processing certain particles (typically e^+/e^-), or by rejecting tracks that may not be visible (i.e. in a shadow region). It can also be used to “slice” simulations in terms of particle energy, atmospheric depth or other parameters.

Formalism The *Formalism* implements the specific radio emission calculation and orchestrates the core calculation. We have fully implemented two formalisms that calculate the electric field vector, namely the CoREAS algorithm [2] which implements the “Endpoints formalism” [4, 5] and the “ZHS” algorithm [7]. Both have been ported as closely as possible from their original

implementations in the CoREAS [2] and ZHAireS [8] air shower simulation codes to allow for direct comparison before we investigate potential refinements.

Propagator The *Propagator* is used by the *Formalism* and *Filter* to calculate the (potentially multiple) valid radio signal propagation paths from each particle track to each antenna. We have already implemented two propagators that use a straight-ray approximation (akin to C7 and ZHAireS) including: 1) an analytic ray path solver that can only be used in media with uniform or exponential refractive indices; and 2) an *integrating* propagator that numerically integrates the time delay along each propagation path and can therefore work in arbitrarily complex media where no analytic solution exists. By separating the propagation of the radio signals from the emission formalism, C8 allows more advanced propagation techniques (e.g. full raytracing or parabolic equation methods) or more complex simulation scenarios (such as cross-media showers) to be implemented without requiring any modifications to the underlying emission formalisms.

Antenna The *Antenna* instance is storing, processing, and managing an individual antenna in the simulation. Multiple instances of independent antennas can be configured in the simulation and can apply their own unique processing to the received electric field, e.g., apply an antenna response. We currently implement a standard time-domain *perfect* antenna (frequency-domain can also be supported) that has a sample rate, start time, and a time window that is configurable individually for each antenna.

As our radio calculation is a standard *process* that is inserted into C8's *process list*, multiple instances of the radio emission can be simulated for the same shower. This immediately allows for comparing different radio implementations (e.g., comparing CoREAS against ZHS, or time-domain against frequency-domain implementations, etc.) on the exact same underlying shower, removing any uncertainty due to differences in the underlying shower or physics models [9]. In this work, we present the first radio pulses generated using C8 but also compare the CoREAS and ZHS algorithms (as implemented in C8) against reference pulses generated by the CoREAS formalism in C7 and the ZHS formalism in ZHAireS.

3. Validation of the implementation

3.1 Electron in a uniform magnetic field

We begin by validating the “CoREAS” and “ZHS” formalisms in C8 by calculating the synchrotron emission from a relativistic electron undergoing circular motion. Following the calculation in [4], we create a circular track of radius $L = 100$ m in the $x - y$ plane on which a 11.4 MeV electron orbits in vacuum ($n = 1$) within a uniform magnetic field of 3.809 Gauss aligned with the z -axis. The antenna is placed in the far field at a distance $R = 30$ km so that the unit vector from the point of emission to the antenna can be considered constant and lies along the z -axis.

We configure C8 using two different particle tracking (propagation) algorithms: 1) a simple algorithm that is used to connect 100,000 points that were explicitly constructed on a circular path with the proper radius with straight lines (“manual” tracking); and 2) the standard leapfrog integrator included in C8 to propagate particles within a magnetic field (“C8 tracking”). For the C8 tracking algorithm, we inject an electron with the correct energy and run the main C8 cascade

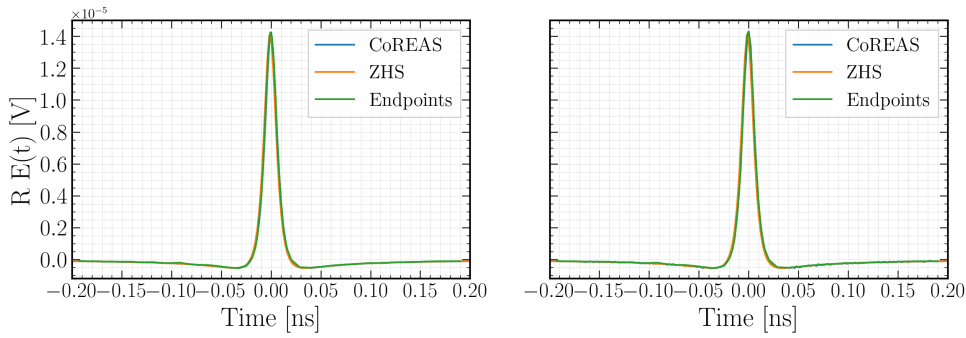


Figure 2: Radio pulse from an electron in a uniform magnetic field performing a circular loop. “Manual tracking” algorithm (left) and “C8 tracking” (right). Both tracking algorithms are compared with the analytical solution of that system presented in [4] - Antenna is set at $R = 30$ km.

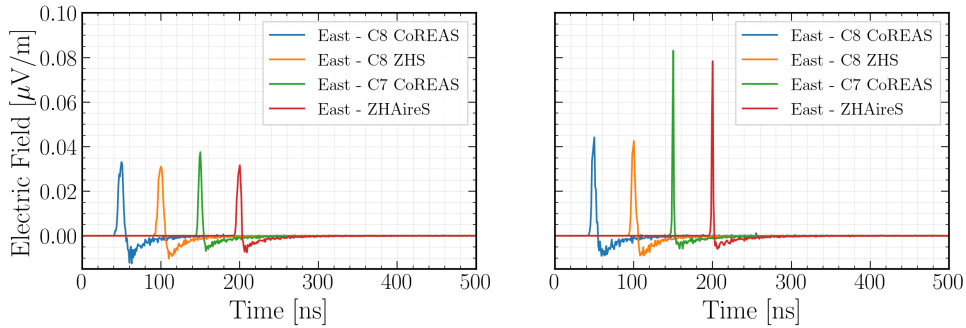


Figure 3: Signal pulse comparison for antenna at 50 m (left) and at 200 m (right) from the shower core. The East polarization of all pulses compared is shown where time offsets are arbitrary.

process for the (analytical) duration it would take for the electron to complete one orbit around its gyroradius. For each case, we simulate each shower with both “CoREAS” and “ZHS” formalisms simultaneously (each is otherwise configured identically). The synchrotron emission calculated by both formalisms is compared against the reference result from [4] in Fig. 2. Both agree extremely well with each other as well as the reference “Endpoints” pulse. We note that we need to configure the C8 tracking to perform very fine steps for accurate calculation of this extremely broad-band pulse.

We thus conclude that both the formalisms and the C8 tracking (for very fine tracking) deliver correct results.

3.2 Simulation of an extensive air shower

We proceed to simulating the radio emission from full extensive air showers using C8. To keep complexity to a minimum, we restrict ourselves to simulating electron-induced showers. We use the “US Standard atmosphere”, a uniform refractive index ($n = 1.000327$), and a constant horizontal geomagnetic field of $50 \mu\text{T}$ aligned in the x direction. We use the standard C8 electromagnetic interaction model (“PROPOSAL” [10]).

We use a 10 TeV vertical shower as the baseline for these comparisons and use a star-shaped grid of antennas on 20 concentric rings spaced equally from 25 m to 500 m from the shower axis with

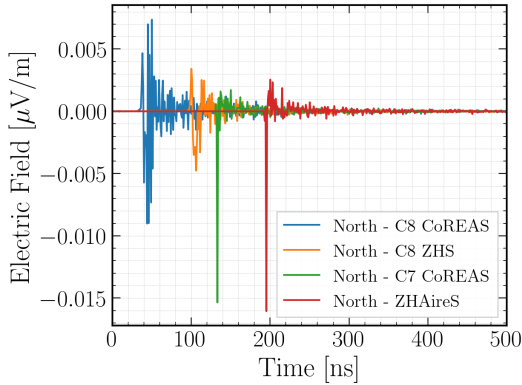


Figure 4: Signal pulse comparison for antenna at 200 m from the shower core - North polarization.

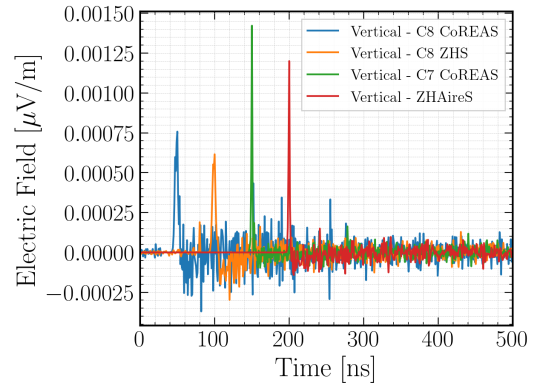


Figure 5: Signal pulse comparison for antenna at 200 m from the shower core - Vertical polarization.

8 antennas distributed azimuthally in each ring (see Fig. 7 for exact antenna locations). The depth of shower maximum of our simulation is $X_{\max} \approx 430 \text{ g cm}^{-2}$. We note that particle energy cuts for electrons and positrons have been set to a comparably high value of 5 MeV because of current limitations in the PROPOSAL version available in the radio branch of C8. Also, the tracking has been specifically configured in C8 to reduce the tracking step size (maximum deviation in the magnetic field of 0.0001 radians) as otherwise the resulting signal traces exhibited high-frequency noise which might point to an issue in the tracking that we still need to investigate in detail.

In Fig. 3 the East polarization of radio pulses calculated for two antennas at 50 m and at 200 m north of the shower axis with the C8-CoREAS and C8-ZHS implementations and compare it with pulses from a similar air shower (similar depth of maximum and number of particles at maximum) simulated with C7 and ZHAireS. The amplitudes for the antennas at 50 m (Fig. 3 left) agree within 12 - 15% between the C8, C7 and ZHAireS implementations. For antennas at 200 m from the shower axis (Fig. 3 right), there is a 50% reduction in signal amplitude in C8 compared to C7 and ZHAireS and as well as a 100% increase in the pulse duration. The C8 pulses are approximately 35% wider for antennas at 50 m and 200 m. The polarization characteristics match very well between the C8 implementations and C7 as well as ZHAireS. This is evident for each polarization individually for the antennas at 200 m in Fig. 3 right (East), Fig. 4 (North) and Fig. 5 (Vertical). There is also very good agreement between C8-CoREAS and C8-ZHS, where the ZHS version exhibits slightly less noise on the pulse.

We also show the frequency spectra for two antennas located inside the Cherenkov ring (50 m and 200 m from the shower axis in Fig. 6). Both formalisms in C8 show an increase in power below $\sim 50 \text{ MHz}$ as compared with C7 and ZHAireS. It is evident that in C8 we are seeing less power at high frequencies with respect to C7 and ZHAireS which might indicate a small issue in time tracking in C8 or the electromagnetic model used; at the same time CoREAS and ZHS are close.

As a final comparison, we calculate and plot 2D maps of the energy fluence in the 30-80 MHz band for both C8 formalisms as well as C7 and ZHAireS in Fig. 7. The absolute scale and polarization characteristics of all results agree qualitatively well, although slight differences become apparent, in particular an offset from the symmetry axis in the $\vec{v} \times (\vec{v} \times \vec{B})$ polarization in the C8 and ZHAireS results which is not present in C7 and a dot in the \vec{v} polarization for only C8 ZHS and ZHAireS.

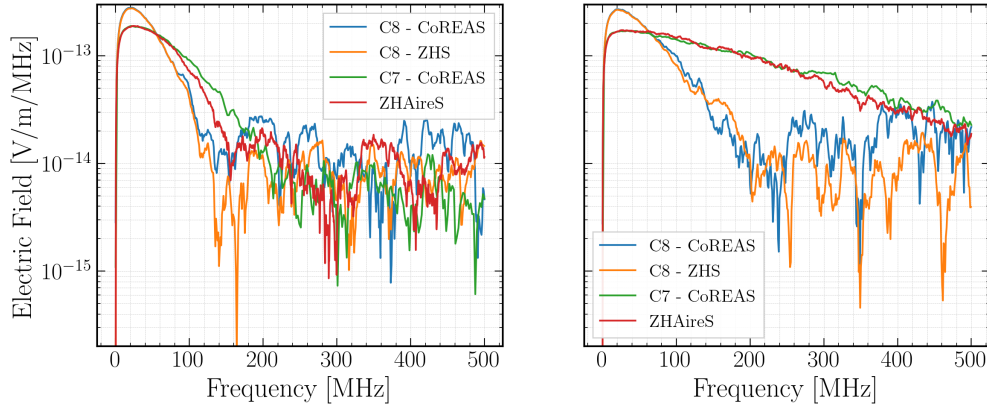


Figure 6: Frequency spectra for antenna at 50 m (left) and at 200 m (right) from the shower core.

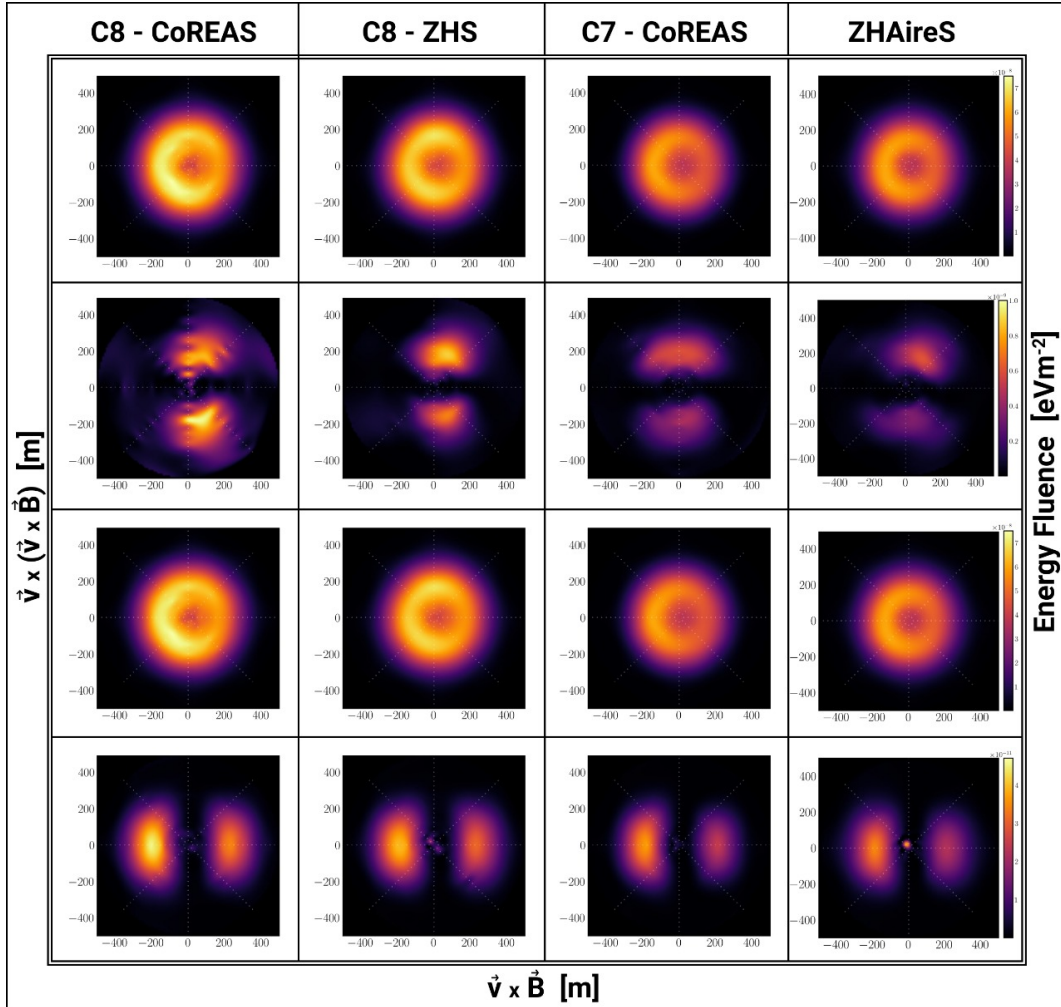


Figure 7: Table of energy fluence in different polarizations of the electric field for C8 CoREAS, C8 ZHS, C7 CoREAS and ZHAireS. The order of the polarizations we see starting from top to bottom is: all polarizations, $\vec{v} \times (\vec{v} \times \vec{B})$, $\vec{v} \times \vec{B}$ and \vec{v} .

4. Conclusions

We have completed a first implementation of radio-emission calculations in C8 based on exact reproductions of the CoREAS and ZHS algorithms implemented in a modern, modular structure that will allow flexible extension for the needs of current and future experiments.

We have performed low-level tests with single electrons undergoing circular motion to establish that the radio-emission calculation as well as the particle tracking in the magnetic field in C8 work correctly. Afterwards, we have performed simulations of a vertical 10 TeV electron shower in a uniform refractive index and compared the results between a reference simulation with C7 as well as ZHAireS and our implementation of the CoREAS and ZHS algorithms in C8. We observe an agreement at the level of better than a factor of two in absolute amplitude, a good agreement of polarization characteristics and a very good agreement between the CoREAS and ZHS implementations in C8. Notably, the radio pulses simulated with C8 are wider and have less high-frequency content.

We note that the air-shower results depend on many ingredients, in particular the underlying electromagnetic interaction model PROPOSAL and the tracking in the magnetic field (which likely needs improvements as we needed to track much finer in C8 than in C7 for instance to achieve comparably clean radio pulses). Having reached this major milestone, we will address the observed differences by detailed studies in the future.

References

- [1] T. Huege, *Phys. Rept.* **620** (2016), 1-52 [1601.07426].
- [2] T. Huege, M. Ludwig and C. W. James, *AIP Conf. Proc.* **1535** (2013) 1, 128 [1301.2132].
- [3] D. Heck, J. Knapp, J.N. Capdevielle, G. Schatz, and T. Thouw, FZKA Report 6019, 1998.
- [4] T. Huege, C. W. James, H. Falcke and M. Ludwig, *Proc. 32nd Int. Cosmic Ray Conf.* (2011) **4**, 308 [1112.2126]
- [5] M. Ludwig and T. Huege, *Astropart. Phys.* **34** (2011), 438-446 [1010.5343]
- [6] R. Engel, D. Heck, T. Huege, T. Pierog, M. Reininghaus, F. Riehn, R. Ulrich, M. Unger and D. Veberič, *Comput. Softw. Big Sci.* **3** (2019) 1, 2 [1808.08226].
- [7] E. Zas, F. Halzen and T. Stanev, *Phys. Rev. D* **45** (1992), 362-376
- [8] J. Alvarez-Muñiz, W. R. Carvalho, Jr., M. Tüeros and E. Zas, *Astropart. Phys.* **35** (2012), 287-299 [1005.0552]
- [9] M. Gottowik, C. Glaser, T. Huege and J. Rautenberg, *Astropart. Phys.* **103** (2018), 87-93 [1712.07442].
- [10] J. M. Alameddine, J. Soedingrekso, A. Sandroock, M. Sackel and W. Rhode, *J. Phys. Conf. Ser.* **1690** (2020) 1, 012021

Acknowledgements

For the simulations presented, computing resources from KIT have been used. This work has also received financial support from Xunta de Galicia (Centro singular de investigación de Galicia accreditation 2019-2022), by European Union ERDF, by the "María de Maeztu" Units of Excellence program MDM-2016-0692, the Spanish Research State Agency and from Ministerio de Ciencia e Innovación PID2019-105544GB-I00 and RED2018-102661-T (RENATA).

Electromagnetic Shower Simulation for CORSIKA 8

Jean-Marco Alameddine,^{a,*} Jaime Alvarez-Muñiz,^b Juan Ammerman-Yebra,^b Lars Bollmann,^a Wolfgang Rhode,^a Maximilian Sackel,^a Alexander Sandrock,^c Jan Soedingrekso^a and Enrique Zas^b on behalf of the CORSIKA 8 Collaboration
(a complete list of authors can be found at the end of the proceedings)

^a*Technical University Dortmund,*

Otto-Hahn-Str. 4a, 44227 Dortmund, Germany

^b*Instituto Galego de Física de Altas Enerxías (IGFAE),*

Universidade de Santiago de Compostela, 15782 Santiago de Compostela, Spain

^c*National Research Nuclear University MEPhI (Moscow Engineering Physics Institute),*

Kashirskoe shosse 31, 115409 Moscow, Russia

E-mail: jean-marco.alameddine@udo.edu

Extensive air showers in astroparticle physics experiments are commonly simulated using CORSIKA. The electromagnetic shower component has been treated using EGS4 in the Fortran 77-based versions, which have been developed in the last thirty years. Currently, CORSIKA is being restructured and rewritten in C++, leading to the new version CORSIKA 8. In this process, the electromagnetic component is now being treated by the high-energy lepton and photon propagator PROPOSAL. Originally designed for the efficient simulation of high-energy muons and tau-leptons in large volume neutrino telescopes, the Monte Carlo library PROPOSAL has been extended to also treat electrons, positrons, and high-energy photons. Validating this new implementation of the electromagnetic shower model is very important. In this talk, the electromagnetic shower component simulated with PROPOSAL is compared to previous versions of CORSIKA, the air shower simulator AIRES as well as the electromagnetic shower tool ZHS, which is optimized for the radio signal. This includes comparisons of the underlying theoretical models as well as lateral and longitudinal shower characteristics, especially of parameters relevant for the radio component such as the charge excess.

37th International Cosmic Ray Conference (ICRC 2021)

July 12th – 23rd, 2021

Online – Berlin, Germany

*Presenter

1. Introduction

For decades, many astroparticle experiments have simulated extensive air showers using CORSIKA [1]. In recent years, a major effort has been started to rewrite CORSIKA in modern C++, resulting in the new version CORSIKA 8. In the course of this undertaking, the propagation of electromagnetic particles has been transferred from a modified version of EGS4 [2] to the PROPOSAL library [3–5]. This contribution is dedicated to the systematic comparison of electromagnetic showers simulated in the current version of CORSIKA 8 to established frameworks, including CORSIKA 7, the air shower simulation program AIRES [6] and the electromagnetic cascade simulation code ZHS MC [7]. In the past, AIRES and ZHS MC have already been compared against GEANT4 and have been found to be in good agreement for simulations in homogeneous ice [8].

This proceeding is divided in two main parts. In Section 2 we compare the theoretical description of the electromagnetic interaction processes in the different codes. Section 3 describes the results of our simulations and compares the longitudinal and lateral shower development as well as the track lengths of simulated showers.

2. Comparison of theoretical descriptions of EM processes

The comparison of the theoretical models used in the different shower frameworks includes energy loss cross sections as well as the scattering models. A discussion is presented of the different treatments of energy thresholds to remove low energetic particles and of cuts to decide whether interactions are treated stochastically or as contributing to the continuous energy loss.

In all frameworks but AIRES, the electromagnetic model is similar to the Electron Gamma Shower code system EGS4 [2]. While in ZHS MC and PROPOSAL, the models are mainly based on EGS4, CORSIKA 7 uses EGS4 directly in a modified version. For AIRES, electromagnetic processes are based on several parametrizations different from EGS, which will be described in more detail later in this chapter. Since EGS4 is a built-in system producing the showers with limited access for external frameworks, the lepton propagator PROPOSAL is being used in CORSIKA 8 as an external library. Thereby, PROPOSAL provides the physical description of the electromagnetic shower component, while the overall task of the shower generation remains in the CORSIKA framework.

The two dominating processes in an electromagnetic shower are electron-positron pair production by photons and bremsstrahlung losses of electrons and positrons. In CORSIKA 7, the bremsstrahlung parametrization of Koch & Motz [9] is used for energies above 50 MeV, while for lower energies, tabulated empirical corrections are applied. The same bremsstrahlung parametrization has been implemented in PROPOSAL. In ZHS MC, the parametrization of Stanev & Vankov [10] is used, which is based on [11, 12], with corrections at low energies from [9]. The framework AIRES uses a cross section based on a parametrization by Rossi & Greisen [13]. In all frameworks, the LPM effect is included, although it can currently not be used in CORSIKA 8.

The same formalism to parametrize the bremsstrahlung cross section is also used for the pair production cross section, except for CORSIKA 8, where a parametrization by Tsai is used [14]. Using two different parametrizations to describe the bremsstrahlung and pair production processes

in CORSIKA 8 is not entirely consistent, however, interchanging the pair production cross section resulted in negligible differences compared to other uncertainties.

Regarding ionization and the production of knock-on electrons, CORSIKA 7, CORSIKA 8 and ZHS MC all use the Berger & Seltzer parametrization [15] of the Bhabha and Møller scattering for electrons and positrons, respectively. In AIRES, a fit to GEANT3 calculations with a distinction between continuous and discrete losses at an energy of 1 MeV is made. For a better comparison with the other frameworks, its continuous energy loss has been substituted by that of Berger & Seltzer [15]. All frameworks also include density correction effects.

Further interactions implemented in all frameworks are the annihilation of positrons with atomic electrons and Compton scattering of photons. Together with Møller and Bhabha scattering, they are relevant for the charge excess of an air shower, and therefore the radio signal [7].

Only in CORSIKA 7 and AIRES, the photohadronic and the photoelectric effects are implemented. For this work, the photohadronic interaction has been deactivated in AIRES to compare only the purely electromagnetic component of the showers. In CORSIKA 7, the photoelectric effect also includes the fluorescence loss. Further processes that are only taken into account by CORSIKA 7 are coherent Rayleigh scattering and the production of muon pairs induced by photons.

In PROPOSAL, the production of electron-positron pairs induced by leptons colliding with nuclei as well as inelastic nuclear interactions are also implemented. The latter, however, is only included as an energy loss process, but not yet as a source of hadronic secondary particles.

For the description of multiple scattering, the Highland approximation [16] of Molière theory is used in all frameworks. The deflection of particles in stochastic interactions is included in CORSIKA 7. These effects are also available in PROPOSAL, but not yet implemented in the interface to CORSIKA 8. In AIRES, Coulomb scattering is implemented as a deflection process.

Besides the physical models, the implementation and treatment of energy cuts are important to compare the simulations. The cuts can be divided into a particle energy cut below which particles are not further propagated. Furthermore, there are energy loss cuts defining the energy above which losses are treated stochastically, while below the cut, they are treated as a continuous energy loss between two interactions.

In AIRES, the user can define particle cuts which need to be above a kinetic energy of 80 keV for the particles in an electromagnetic shower. Energy loss cuts are set in the code and can not be changed externally. For this work, the AIRES code has been modified in such a way that the energy loss cuts match those used in the other frameworks. In ZHS MC, energy cuts are carefully linked to the cut between discrete and continuous losses, without an option to change them individually. For comparison reasons, an independent particle cut has been introduced in an attempt to match the cross sections and the same integration limits of the other frameworks. Since the particle cuts in AIRES and ZHS MC have been modified from their initial values, these routines may not perform with their optimal accuracy.

In CORSIKA 7, the particle cuts can be changed as long as they are above 10 keV for electrons and positrons, and above 1 keV for photons. The energy loss cut can not be set in CORSIKA 7. In CORSIKA 8, both the energy loss cut and the particle cut can be adjusted independently for the different particle types. For comparison reasons, all particle cuts have been set to 4 MeV and energy loss cuts to half of the particle cut since CORSIKA 8 is known to produce stable results for these settings.

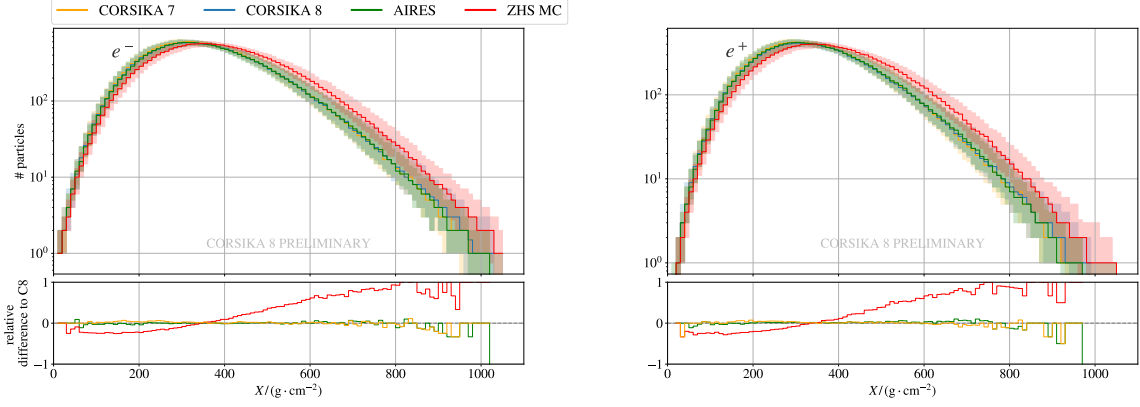


Figure 1: Longitudinal profile for 200 showers initiated by 1 TeV electrons. The relative difference to CORSIKA 8 is defined as $\frac{m - m_{C8}}{m_{C8}}$ with the median m of the particle number.

3. Comparison of simulated shower parameters

To validate the current status of the simulations of the electromagnetic shower component in CORSIKA 8 using PROPOSAL, relevant shower observables are calculated and compared to the results from simulations created with other shower simulation codes. These comparisons are vital to understand the current status of CORSIKA 8, but also to highlight the remaining limitations when interpreting the physical results which are obtained with it.

For the results presented in this contribution, we used version 7.7410 of CORSIKA 7 [1], version 19.04.00 of AIRES [6], the release tagged `icrc-2021` for CORSIKA 8 [17] and the most recent version of ZHS MC [18]. All the comparisons that are presented have been obtained by simulating an electromagnetic shower induced by an electron with an initial energy of 1 TeV. The particle threshold has been set to 4 MeV, i.e. shower particles with a kinetic energy below this threshold are discarded. The energy loss cuts have been set to 2 MeV for photons and to 2.255 MeV for electrons and positrons.

For CORSIKA 7, all simulations have been made using the U.S. Standard Atmosphere model, an inhomogeneous density profile of the atmosphere. For ZHS MC, all air showers were simulated in a homogeneous atmosphere, as this is the only option available, with a density of 1200 g m^{-3} . CORSIKA 8 and AIRES simulations were run for both inhomogeneous and homogeneous atmospheres. Since there are no particles decaying in purely electromagnetic showers, we do not expect this to significantly affect the comparisons of the longitudinal shower development in terms of grammage.

3.1 Longitudinal shower development

The longitudinal shower development is analyzed by counting the total number of particles crossing planes along the shower axis and perpendicular to it. This is shown for the different particle types in Figure 1, where the longitudinal profile has been calculated using the simulations of 200 showers. Here, the solid lines indicate the median, while the shaded bands display the interquartile range of the particle number.

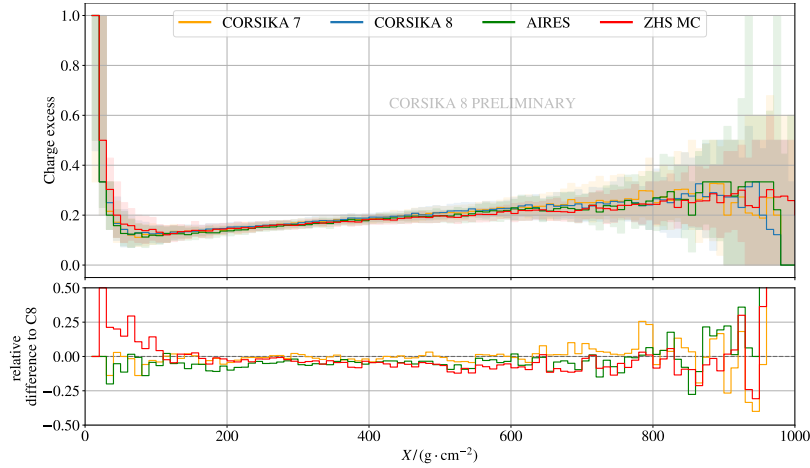


Figure 2: Longitudinal distribution of the charge excess, defined as $\frac{N_{e^-} - N_{e^+}}{N_{e^-} + N_{e^+}}$, for 200 showers initiated by 1 TeV electrons.

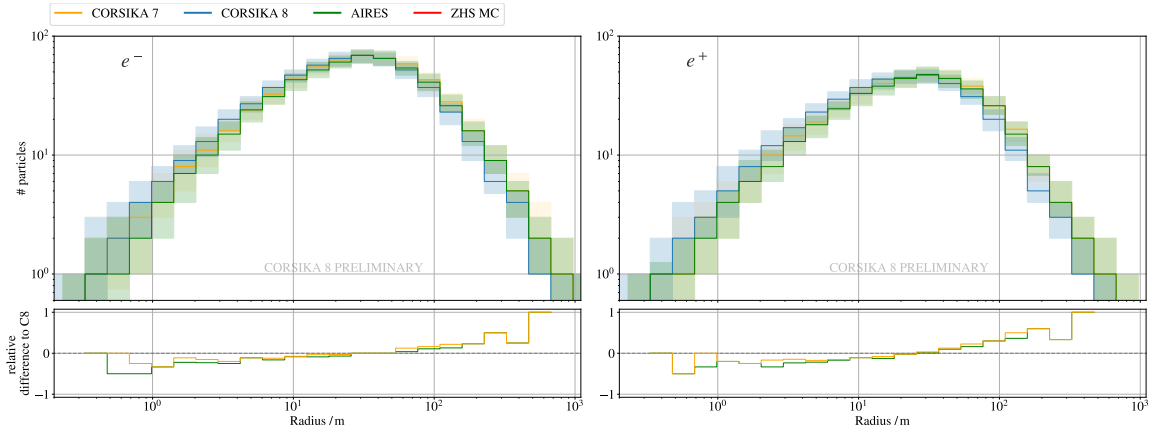
While the general shapes of the longitudinal shower distribution agree, a displacement of the showers simulated with ZHS MC towards larger depths is clearly visible. For CORSIKA 7, CORSIKA 8 and AIRES, the medians of the distribution all agree within 5 %.

Figure 2 shows the longitudinal development of the difference between the electron and positron number, called charge excess. This effect is caused by the ionization of atomic electrons either by charged leptons or by Compton scattering as well as by annihilation of positrons. The resulting charge excess is, together with the geomagnetic contribution, a mechanism for radio emission in air showers, and shows an agreement between the different frameworks that is within 10 % around the depth of the shower maximum.

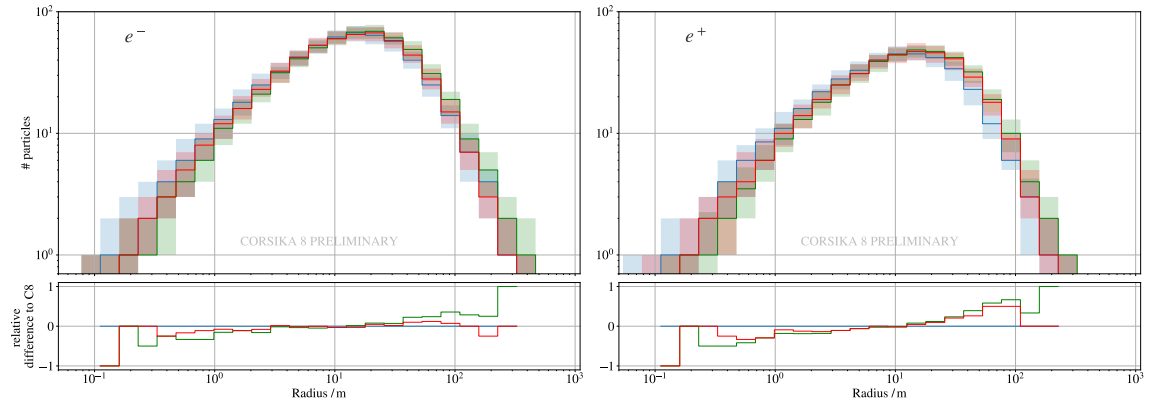
3.2 Lateral shower development

The lateral shower development, i.e. the distribution of the shower perpendicular to the shower axis, is computed by selecting all particles passing a given observation level and calculating their distance to the shower axis. The resulting lateral particle distribution of electrons and positrons is shown for simulations in an inhomogeneous atmosphere in Figure 3a, and for simulations in a homogeneous atmosphere in Figure 3b. For the inhomogeneous medium, the observation level has been set to 8600 m above sea level, which corresponds to an atmospheric depth of approximately 335 g cm^{-3} , while for the homogeneous medium, the observation level has been set directly to the shower maximum. The median number of particles is depicted by the solid lines, the shaded bands indicate the interquartile range of the particle number.

The comparisons show that in both the inhomogeneous and homogeneous atmosphere, the lateral profiles from the CORSIKA 8 simulations are shifted slightly closer to the shower axis compared to the simulations done with the other frameworks. This indicates that showers produced by CORSIKA 8 have a smaller lateral spread, which can be understood since not all contributing processes have yet been implemented in CORSIKA 8. For example, bremsstrahlung photons produced by electrons and positrons inherit the direction of the initial lepton, neglecting the photon emission angle.



(a) Distributions for an observation height of 8600 m in an inhomogeneous atmosphere.



(b) Distributions for an observation height at the shower maximum in a homogeneous atmosphere.

Figure 3: Lateral particle distributions for 200 showers initiated by 1 TeV electrons.

3.3 Shower track lengths

For our purposes, the track length is defined as the sum of the lengths of all electron and positron tracks, with the projected track length defined as the sum of all tracks projected onto the shower axis. Both quantities are calculated for 200 showers in both homogeneous and inhomogeneous atmospheres, simulated with the different frameworks.

In addition, the excess track length is calculated, which is the sum of all electron track lengths in the shower minus the sum of all positron track lengths, while the projected excess track length is defined analogously to the projected charged track length. The projected excess track length is an important quantity in simulating the radio emission of air showers, as it is the quantity that establishes the normalization of the electric field spectrum [7]. The distributions of the projected excess track lengths are shown in Figure 4, the medians and standard deviations of all track length observables are presented in Table 1. Notably, the standard deviation of the total and projected track length of the CORSIKA 8 simulation in homogeneous media is, compared to the other frameworks, increased by two orders of magnitude. This is due to an outlier in the simulation with a very small track length, caused by a photonuclear interaction whose secondary particles are currently not further propagated. Otherwise, the medians of the observables all agree on a 10% level.

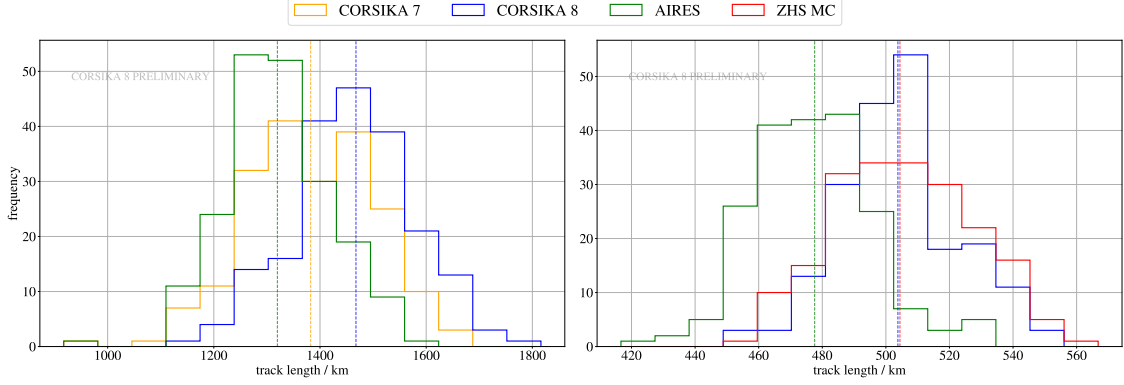


Figure 4: Distribution of the excess charged track length, i.e. the difference between the sum of all electron track lengths projected onto the shower axis and the sum of all positron track lengths projected onto the shower axis, for 200 showers initiated by 1 TeV electrons. The left plot shows the distribution for an inhomogeneous atmosphere, the right plot for a homogeneous atmosphere. The dashed lines indicate the medians of the corresponding distributions.

Table 1: Track length medians for 200 showers, initiated by 1 TeV electrons, for simulations in inhomogeneous and homogeneous atmospheres. The parentheses indicate the standard deviation.

	inhomogeneous			homogeneous		
	C7	C8	AIRES	C8	AIRES	ZHS MC
Total track / km	8083(724)	7868(642)	8047(620)	2891(202)	2916(3)	3126(2)
Proj. track. / km	7750(697)	7837(640)	7681(594)	2776(194)	2771(3)	2924(2)
Excess / km	1483(129)	1493(115)	1427(106)	549(43)	520(19)	574(22)
Proj. excess / km	1382(121)	1468(113)	1320(99)	504(40)	478(19)	504(22)
Proj. excess / Total	0.171	0.187	0.164	0.174	0.164	0.161

4. Outlook

In this work, the results of the first simulations of electromagnetic showers within the framework CORSIKA 8, using PROPOSAL as an electromagnetic model, have been presented and compared to other shower simulation tools. Although these comparisons revealed several differences, the general results are promising.

Further work on both PROPOSAL and the interface to CORSIKA 8 is necessary in the future. In order to improve the longitudinal distribution, the photohadronic interaction of photons will be implemented. Furthermore, a correct treatment of the LPM effect in inhomogeneous media still needs to be applied. Both additions will be especially relevant for the simulation of higher-energetic showers.

With regard to the lateral distribution, the deflection of primary particles in stochastic interactions as well as the deflection of bremsstrahlung photons will be added in the near future. Including these effects may solve the deviations currently observed in the lateral profile of CORSIKA 8.

Parallel to these improvements, further comparisons to these and other simulation frameworks,

as well as simulations in other media such as ice, are going to be necessary. Since CORSIKA 8 is still in an early development state, runtime comparisons to the other frameworks are not yet conclusive and need to be conducted in future analyses.

Acknowledgments

We acknowledge funding by the Deutsche Forschungsgemeinschaft under the grant numbers RH 25/9-1 (J. S., W. R.) and SA 3867/1-1 (A. S.). This work has been supported by the DFG, Collaborative Research Center SFB 876, project C3 (<http://sfb876.tu-dortmund.de>).

This work has received financial support from Xunta de Galicia (Centro singular de investigación de Galicia accreditation 2019-2022), by European Union ERDF, by the María de Maeztu Units of Excellence program MDM-2016-0692, the Spanish Research State Agency and from Ministerio de Ciencia e Innovación PID2019-105544GB-I00 and RED2018-102661-T (RENATA).

References

- [1] D. Heck et al., *CORSIKA: A Monte Carlo code to simulate extensive air showers*, Tech. Rep. FZKA-6019, Forschungszentrum Karlsruhe, 1998.
- [2] W. R. Nelson, H. Hirayama, and D. W. O. Rogers, *The EGS4 code system*, Tech. Rep. SLAC-265, Stanford Linear Accelerator Center, 1985.
- [3] J.-H. Koehne et al., *Comput. Phys. Commun.* **184** (2013) 2070–2090.
- [4] M. Dunsch et al., *Comput. Phys. Commun.* **242** (2019) 132–144.
- [5] J.-M. Alameddine et al., *J. Phys. Conf. Ser.* **1690** (2020) 012021.
- [6] S. J. Sciutto, *AIRES - A system for air shower simulations*, 2019.
- [7] E. Zas, F. Halzen, and T. Stanev, *Phys. Rev. D* **45** (1992) 362–376.
- [8] J. Alvarez-Muñiz, W. R. Carvalho, Jr., M. Tüeros, and E. Zas, *Astropart. Phys.* **35** (2012) 287–299.
- [9] H. Koch and J. Motz, *Reviews of modern physics* **31** (1959) 920.
- [10] T. Stanev and C. Vankov, *Comput. Phys. Commun.* **16** (1979) 363–372.
- [11] J. C. Butcher and H. Messel, *Phys. Rev.* **112** (1958) 2096–2106.
- [12] J. C. Butcher and H. Messel, *Nucl. Phys.* **20** (1960) 15–128.
- [13] B. Rossi and K. Greisen, *Rev. Mod. Phys.* **13** (1941) 240–309.
- [14] Y.-S. Tsai, *Rev. Mod. Phys.* **46** (1974) 815.
- [15] S. M. Seltzer and M. J. Berger, *Int. J. Appl. Radiat. Isot.* **33** (1982) 1219–1226.
- [16] V. L. Highland, *Nuclear Instruments and Methods* **129** (1975) 497–499.
- [17] M. Reininghaus and R. Ulrich, *EPJ Web Conf.* **210** (2019) 02011.
- [18] J. Alvarez-Muñiz, E. Marqués, R. A. Vázquez, and E. Zas, *Phys. Rev. D* **74** (2006) 023007.

Air shower genealogy for muon production

Maximilian Reininghaus,^{a,b,*} Ralf Ulrich^a and Tanguy Pierog^a

^aKarlsruher Institut für Technologie (KIT), Karlsruhe, Germany

^bInstituto de Tecnologías en Detección y Astropartículas (ITeDA), Buenos Aires, Argentina

E-mail: reininghaus@kit.edu

Measurements of the muon content of extensive air showers at the highest energies show discrepancies compared to simulations as large as the differences between proton and iron. This so-called muon puzzle is commonly attributed to a lack of understanding of the hadronic interactions in the shower development. Furthermore, measurements of the fluctuations of muon numbers suggest that the discrepancy is likely a cumulative effect of interactions of all energies in the cascade. A feature of the air shower simulation code CORSIKA 8 allows us to access all previous generations of final-state muons up to the first interaction. With this technique, we study the influence of interactions happening at any intermediate stage in the cascade on muons depending on their lateral distance in a quantitative way and compare our results with predictions of the Heitler–Matthews model.

37th International Cosmic Ray Conference (ICRC 2021)
July 12th – 23rd, 2021
Online – Berlin, Germany

*Presenter

1. Introduction

Muons in extensive air showers (EAS) induced by cosmic rays (CR) are for the most part the end product of the hadronic cascade: long-lived, high energy hadrons interact with nuclei of air molecules (mainly ^{14}N and ^{16}O), producing hadrons of lower energy which eventually decay to muons after several generations of interactions. Therefore, muon observables provide valuable probes of hadronic interactions up to the highest energies. Regarding the total number of muons N_μ , a discrepancy has been found between EAS simulations using state-of-the-art hadronic interaction models and measurements by several experiments [1, 2]. As the meta-analysis ref. [1] shows, this muon deficit (referring to an underestimation of N_μ in simulations) is present at $\sim 10^{17}$ eV, which corresponds to LHC energy in the center-of-mass frame, and increases with primary energy. It poses a major obstacle to inferring the mass composition of ultra-high energy cosmic rays (UHECR) from N_μ . On the other hand, a recent measurement of the fluctuations of N_μ at the Pierre Auger Observatory shows good agreement between simulations and data [3]. Considering that this observable is dominated by the first few interactions in the shower, one can reason that the cause of the muon deficit is likely the effect of accumulating small deviations over several generations covering many orders of magnitude in energy. To determine which features of hadronic interaction models are good candidates for tweaking to enhance the muon production, it is beneficial to quantify the relevance of different phase-space regions of hadronic interactions: projectile species, \sqrt{s} , and kinematic distributions of their produced secondaries.

A similar study has been conducted by Hillas [4] with the computational resources and tools (the EAS simulation code MOCCA) available at that time. A crucial ingredient of this study was the ability to record and inspect the lineage of particles reaching ground, i.e. the mother, grandmother, etc. particles up to the primary. In contrast to MOCCA and somewhat surprisingly, none of the more recent EAS simulation codes AIRES [5], CONEX [6] and CORSIKA [7], which remain the most widely used ones up until today, provide this feature to the required extent. Nevertheless, in AIRES and CORSIKA [8] mother and grandmother particles are accessible, which allows to relate the last hadronic interaction in which a secondary meson is produced that subsequently decays into the muon with that muon [9].

For the currently being developed EAS simulation code CORSIKA 8 [10] we designed and implemented an algorithm capable of retaining the complete lineage of each particle. The information available about any ancestor particle include the type of event in which the particle was produced (decay or interaction), the state of the projectile (position, 4-momentum) of that event and the state of all secondaries. It is also foreseen (though not implemented yet) to include dynamical meta-information of events. For example, for hadronic interactions it may be desirable to save quantities like the number of wounded nucleons, elasticity or whether or not the interaction was diffractive. A more detailed technical description is given in ref. [11].

In this work, we make use of this feature in simulations of UHECR-induced EAS (10^{17} eV and above) with CORSIKA 8 to study hadronic interactions happening throughout the whole shower development with respect to final-state muons on ground.

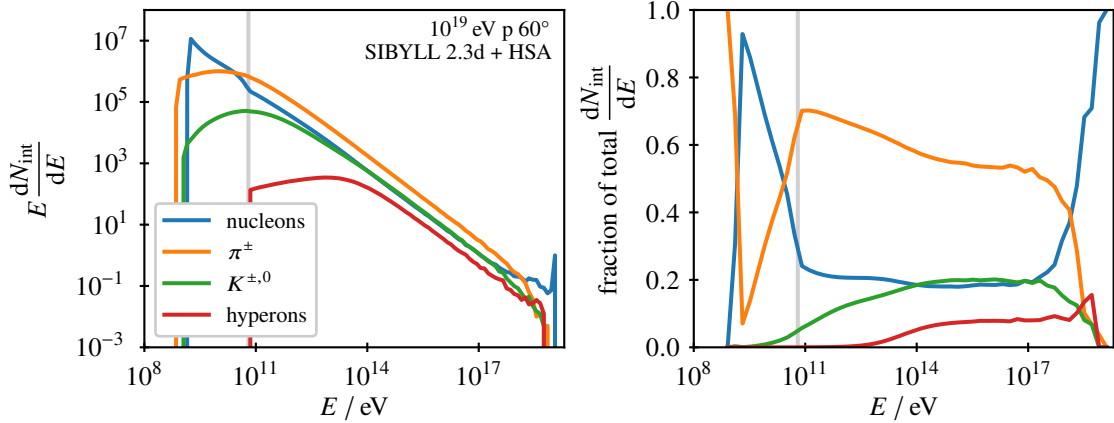


Figure 1: Number of hadronic interactions by energy and species. The grey vertical line indicates the transition between low- and high-energy interaction models.

2. Methods

We simulate EAS with a hybrid approach. We use CORSIKA 8 for a Monte Carlo treatment of the hadronic and muonic shower components, while electromagnetic (EM) particles, mainly the product of π^0 and μ^\pm decays, are fed into CONEX to generate EM longitudinal profiles by numerically solving the cascade equations. Photo-production of hadrons is not taken into account. We use the hadronic interaction models SIBYLL 2.3d [12] and QGSJetII-04 [13] for energies above $10^{1.8}$ GeV = 63.1 GeV. Below that energy and down to the cutoff of 631 MeV kinetic energy we use the Hillas splitting algorithm (HSA) [14] as implemented in an extended version in AIRES 19.04.00 [5] that we link to. The inelastic cross-sections in this energy range are taken from tabulated values that are part of the UrQMD [15] distribution in CORSIKA 7. The atmospheric model used is that of Linsley (see e.g. ref. [16]). The observation level is placed at 1400 m a.s.l. All data presented are averaged over 400 showers.

3. Results

3.1 Interaction spectrum

Figure 1 shows the *interaction spectrum*, i.e. the number of hadronic interactions by energy, of a 10^{19} eV proton shower of 60° zenith angle, grouped by several classes of hadrons. This observable is related to the corresponding energy spectra by

$$\frac{dN_{\text{int}}}{dE} = \frac{1}{\lambda_{\text{int}}(E)} \int dX \frac{dN}{dE}. \quad (1)$$

The interaction spectrum of a given particle species is mainly influenced by the multiplicity of this species as secondaries in hadronic interactions, as well as its critical energy.

Going from high to low energies, we first observe a peak at the primary energy, which in the limit of infinitesimal bin widths would be a delta function. For about one decade in energy

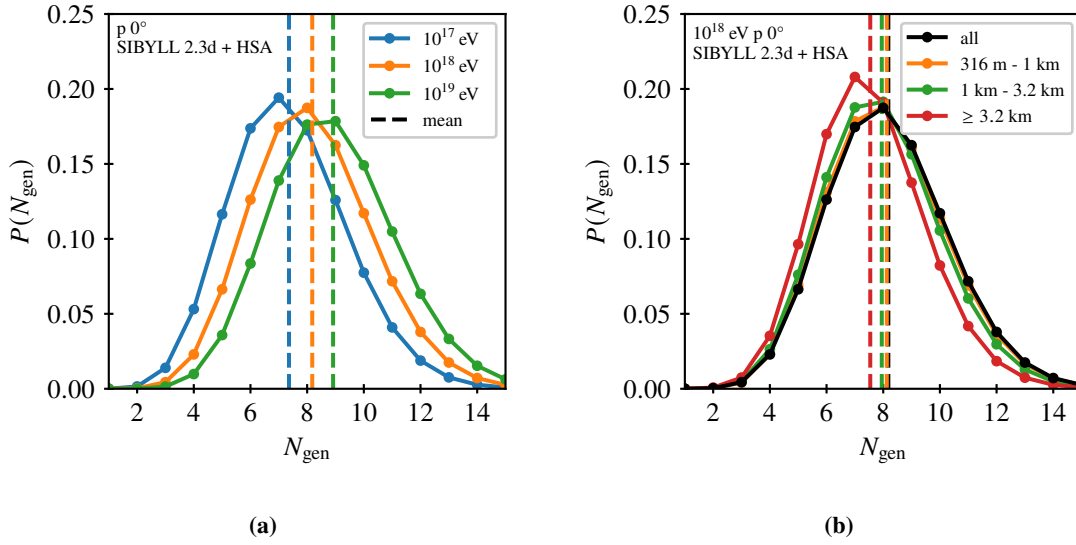


Figure 2: Number of muon ancestor generations (a) by primary energy (b) grouped by radial ranges around shower core. Vertical dashed lines indicate the mean value of the distribution of the same colour.

below the primary energy, most interactions are those of nucleons, which can be attributed to the leading nucleons of the primary interaction. Below the crossing point, pion-air interactions are the dominating component, making up 50 % to 70 % of all hadronic interactions. Between 10^{14} eV to 10^{17} eV kaons and nucleons contribute equally to the total interaction spectrum with about 20 % each. Below 10^{14} eV, the kaon contribution decreases due to the K_S^0 starting to predominantly decay instead of interacting. At that point also hyperons (mainly $\Lambda/\bar{\Lambda}$, the most long-lived hyperon), which are generally rare and rinteract only to a minor extent at all, fade away almost entirely. For a wide range in energy the total spectrum as well as the individual components follow a power-law. Performing a linear fit of the total $\log(EdN_{\text{int}}/dE)$ vs. $\log E$ in the range 1 TeV to 0.1 EeV, we obtain an exponent of -0.890 ± 0.002 . The individual power-laws of unstable hadrons are broken when the corresponding species reaches its critical energy. Around 100 GeV the most long-lived and down to this energy most abundant π^\pm also start to drop out. The switch from high- to low-energy interaction model causes a sudden change in the nucleon spectra, which is an artifact of the simplified treatment of the HSA. These low-energy nucleon interactions play only a minor role regarding muon production, however, as we will show later.

3.2 Number of generations

In fig. 2 we study the number of generations N_{gen} of ground-reaching muons, which is the total number of hadronic interactions that connect the primary particle with the muon in the shower. It is an important quantity since the number of muons grows exponentially with N_{gen} [17, 18] and small changes in hadronic interactions, e.g. the energy fraction transferred from the projectile onto further long-lived hadronic secondaries, are correspondingly amplified N_{gen} times by the multiplicative process [19, 20]. Making use of the lineage technique, N_{gen} is obtained by iterating over the muon ancestors and counting only interaction events (in contrast to decays). Figure 2a shows the distributions for different primary energies. The mean value grows logarithmically with the primary

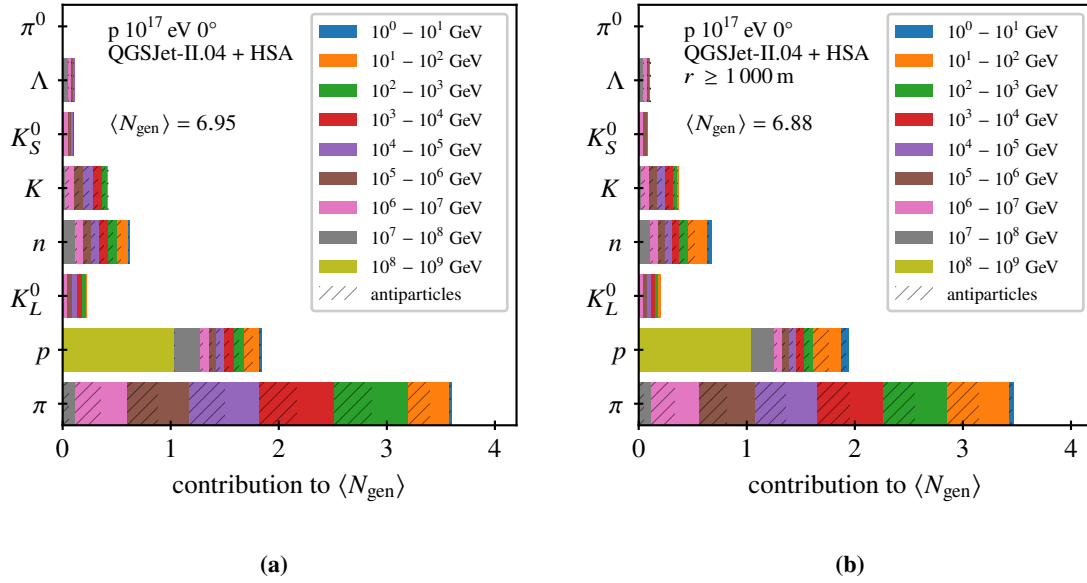


Figure 3: Distribution of muon ancestor projectile generations by energy and species (a) all muons (b) only muons with $r \geq 1000$ m.

energy as expected from the Heitler–Matthews model [17]. A linear fit of $\langle N_{\text{gen}} \rangle$ vs. $\log_{10}(E)$, in which we include also data of $10^{17.5}$ eV and $10^{18.5}$ eV showers not shown in the plot, yields an increase of N_{gen} of $s = 0.785 \pm 0.017$ per decade of energy. In the Heitler–Matthews model, s is related to the hadron multiplicity m via $s = 1/\log_{10}(m)$, so that we can derive $m = 18.8 \pm 1.2$. In fig. 2b we consider only muons within certain radial ranges r around the shower core. We observe that muons further away from the core tend to have slightly fewer generations than those close to the core.

It is instructive to quantify to which degree interactions in certain energy ranges and with certain projectiles contribute to the total N_{gen} . A priori we can only state the obvious: The first interaction, being the root of the shower, contributes exactly one generation. We build a histogram binned in projectile energy and species by iterating over the muon lineages and filling the histogram for each interaction according to its projectile energy and species. Thereby each muon increases the total histogram count by its individual N_{gen} . Since muons share parts of their lineage, the corresponding interactions are counted multiple times – their *muon weight* is given by the number of muons stemming from that interaction. If we finally divide the bin counts by the total number of muons (possibly after applying a section criterion, e.g. on r), we end up with that bin’s contribution to $\langle N_{\text{gen}} \rangle$. The result of that procedure is shown in fig. 3, applied to 10^{17} eV showers. As expected, the bin containing solely the primary interaction (■-coloured) has a value of one. In the energy decade below the primary energy, the main contribution is due to nucleons with about twice as many protons as neutrons, conforming with fig. 1. In this energy range virtually no contribution of antinucleons is apparent. Charged pions contribute approximately half of the total $\langle N_{\text{gen}} \rangle$. Each $\log E$ range between 10 PeV and 100 GeV carries comparable weight, slightly decreasing with energy. No distinction between positively and negatively charged pions can be observed. Below 100 GeV the importance of pion interactions decreases again as more and more

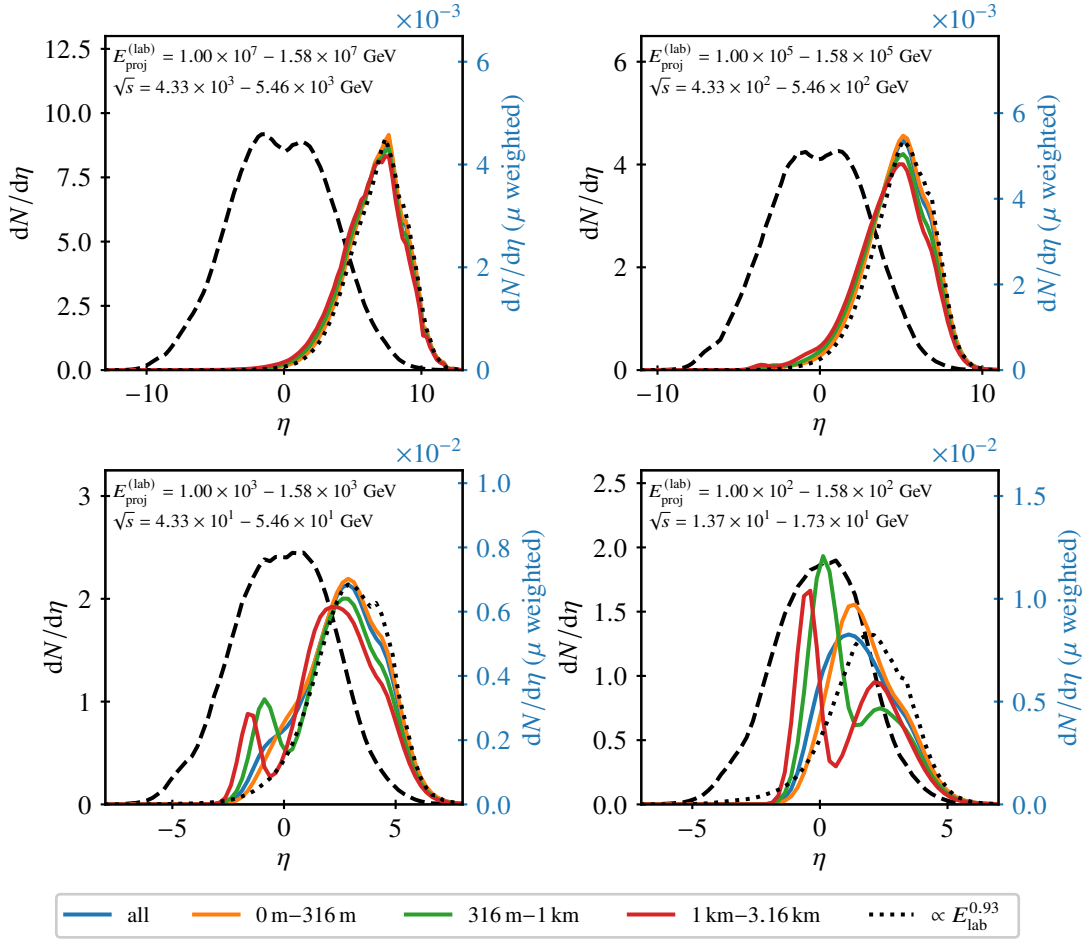


Figure 4: Pseudorapidity distributions of $\pi^\pm + \text{Air} \rightarrow \text{charged hadrons}$, 10^{19} eV vertical proton. The dashed line indicates generator-level distributions while the coloured and dotted lines shows muon-weighted distributions (in arbitrary units).

pions do not reinteract. Comparing the distributions obtained when selecting only muons with at least 1 km lateral distance (fig. 3b) with those without any cut (fig. 3a), we find that for great lateral distance the importance of low-energy interactions increases. This can be understood considering that typically muons with higher energies stay close to the shower core. As the projectile energy of the last interaction of these muons needs to be higher than the final muon energy, the phase space that can contribute to these muons is necessarily cut off earlier.

3.3 Pseudorapidity distributions

To quantify the importance of different regions of the phase-space of secondaries in hadronic interactions for muon production, one may weight specific phase-space element by the number of muons descending from particles produced in it. A simple prescription based on the Heitler–Mathews model is to weight by E_{lab}^β (with $\beta = 0.93$, E_{lab} is the energy of the secondary in the lab frame) [18, 20]. This, however, does not allow for any cut to be applied on the muons, e.g. on lateral distance. Having the full lineage available in our Monte Carlo simulations, we follow the

approach of Hillas [4] and obtain the weight by counting the muons as described in the previous section. In fig. 4, we show pseudorapidity distributions $dN/d\eta$ of $\pi^\pm + \text{Air} \rightarrow \text{charged hadrons}$ (in center-of-mass frame) for four different energies. The pure generator-level distributions (generated with SIBYLL 2.3d in CRMC [21] for a fixed projectile energy E_p and ^{14}N target) are plotted with dashed lines. The corresponding muon-weighted distributions are obtained from simulations of vertical 10^{19} eV proton showers in which we consider interactions within a range around E_p . The solid, coloured lines indicate the weighted distributions (in arbitrary units) after applying a lateral distance cut and normalized by the number of muons selected. Additionally, the black solid line shows the E_{lab}^β -based weighting for comparison. We find that at lab energies $\gtrsim 10^{14}$ eV the weighted distributions almost coincide irrespective of the muon lateral distance. Furthermore, the E_{lab}^β -based weight agrees very well with the distributions (up to an arbitrary scaling factor). These results quantitatively demonstrate the importance of the forward region of hadronic interactions for muon production. At lower energies, on the other hand, the muon lateral distance has an impact on the corresponding weight distributions. Besides the peak in the forward region, a second peak at mid-rapidity around $-2 \lesssim \eta \lesssim 0$ emerges when only muons with at least a few hundred meters distance are considered, which is not described by the E_{lab}^β -based weighting.

4. Conclusions

In this work, we have studied the lineage of muons in air shower simulations of UHECR protons, consisting of hadronic interactions. We have shown that the average number of generations N_{gen} grows logarithmically with the primary energy in accordance with the Heitler–Matthews model. For large lateral distances, the distribution of N_{gen} shift towards lower values. The typical muon lineage contains at energies close to the primary energy mostly interactions of nucleons. The remaining energy range is dominated by pion interactions. Furthermore, we have applied a "muon-weighting" to pseudorapidity distributions of pion-air interactions, showing the importance of the forward region in a quantitative manner for high energy interactions. At lower center-of-mass energies, say $\sqrt{s} \lesssim 100$ GeV, and especially for muons at large lateral distances also the region at lower values of η becomes more and more relevant.

Accelerator measurements conducted in a much more controlled environment that cover the relevant phase-space and emulate the interactions in EAS as closely as possible are key ingredients to constrain the hadronic interaction models better. Fixed-target experiments such as NA61/SHINE with π^\pm beams are especially relevant to study the last generation of hadronic interactions. Complementary to that are LHC measurements, ideally of proton-oxygen collisions [22], which constrain the most energetic interactions in ultra-high energy EAS. Here, data of forward measurements are highly valued input.

Acknowledgments

The simulations were performed on the bwForCluster BinAC of the University of Tübingen, supported by the state of Baden-Württemberg through bwHPC and the DFG through grant no. INST 37/935-1 FUGG.

References

- [1] H. P. Dembinski et al. (EAS-MSU, IceCube, KASCADE-Grande, NEVOD-DECOR, Pierre Auger, SUGAR, Telescope Array, Yakutsk EAS Array), *EPJ Web Conf.* **210**, 02004 (2019), [arXiv:1902.08124 \[astro-ph.HE\]](#).
- [2] F. Gesualdi, A. D. Supanitsky, and A. Etchegoyen, *Phys. Rev. D* **101**, 083025 (2020), [arXiv:2003.03385 \[astro-ph.HE\]](#).
- [3] A. Aab et al. (Pierre Auger), *Phys. Rev. Lett.* **126**, 152002 (2021), [arXiv:2102.07797 \[hep-ex\]](#).
- [4] A. M. Hillas, *Nucl. Phys. B Proc. Suppl.* **52**, 29–42 (1997).
- [5] S. J. Sciutto, *10.13140/RG.2.2.12566.40002* (1999), [arXiv:astro-ph/9911331 \[astro-ph\]](#).
- [6] T. Bergmann et al., *Astropart. Phys.* **26**, 420–432 (2007), [arXiv:astro-ph/0606564 \[astro-ph\]](#).
- [7] D. Heck et al., *CORSIKA: A Monte Carlo code to simulate extensive air showers*, tech. rep. FZKA-6019, doi:[10.5445/IR/270043064](#) (Forschungszentrum Karlsruhe, 1998).
- [8] D. Heck and R. Engel, *The EHISTORY Option of the Air-Shower Simulation Program CORSIKA*, tech. rep. FZKA-7495, doi:[10.5445/IR/270078292](#) (Forschungszentrum Karlsruhe, 2009).
- [9] C. Meurer et al., *Czech. J. Phys.* **56**, A211 (2006), [arXiv:astro-ph/0512536 \[astro-ph\]](#).
- [10] R. Engel et al., *Comput. Softw. Big Sci.* **3**, 2 (2019), [arXiv:1808.08226 \[astro-ph.IM\]](#).
- [11] A. A. Alves Jr. et al., in *Proceedings of the 25th International Conference on Computing in High Energy and Nuclear Physics* (2021).
- [12] F. Riehn et al., *Phys. Rev. D* **102**, 063002 (2020), [arXiv:1912.03300 \[hep-ph\]](#).
- [13] S. Ostapchenko, *Phys. Rev. D* **83**, 014018 (2011), [arXiv:1010.1869 \[hep-ph\]](#).
- [14] A. M. Hillas, in *Proc. 17th Int. Cosmic Ray Conf.* (1981), p. 193.
- [15] M. Bleicher et al., *J. Phys. G* **25**, 1859–1896 (1999), [arXiv:hep-ph/9909407 \[hep-ph\]](#).
- [16] J. Cruz Moreno and S. Sciutto, *Eur. Phys. J. Plus* **128**, 104 (2013).
- [17] J. Matthews, *Astropart. Phys.* **22**, 387–397 (2005).
- [18] L. Cazon, R. Conceição, and F. Riehn, *Phys. Lett. B* **784**, 68–76 (2018), [arXiv:1803.05699 \[hep-ph\]](#).
- [19] L. Cazon et al., *Phys. Rev. D* **103**, 022001 (2021), [arXiv:2006.11303 \[astro-ph.HE\]](#).
- [20] J. Albrecht et al., (2021), [arXiv:2105.06148 \[astro-ph.HE\]](#).
- [21] R. Ulrich, T. Pierog, and C. Baus, *Cosmic Ray Monte Carlo Package, CRMC*, version 1.8.0, doi:[10.5281/zenodo.4558706](#), 2021.
- [22] J. Aichelin et al., *CERN Yellow Rep. Monogr.* **7**, edited by Z. Citron et al., 1159–1410 (2019), [arXiv:1812.06772 \[hep-ph\]](#).

Hadron cascades in CORSIKA 8

Ralf Ulrich,^{a,*} Anatoli Fedynitch,^b Tanguy Pierog,^a Maximilian Reininghaus^{a,c} and Felix Riehn^{d,e} on behalf of the CORSIKA8 Collaboration
(a complete list of authors can be found at the end of the proceedings)

^a*Institute for Astroparticle Physics, Karlsruhe Institute of Technology, Germany*

^b*Institute for Cosmic Ray Research, The University of Tokyo, Japan*

^c*Instituto de Tecnologías en Detección y Astropartículas, Buenos Aires, Argentina*

^d*Instituto Galego de Física de Altas Enerxías, Universidade de Santiago de Compostela, Spain*

^e*Laboratory of Instrumentation and Experimental Particles, Lisbon, Portugal*

E-mail: ralf.ulrich@kit.edu

We present characteristics of hadronic cascades from interactions of cosmic rays in the atmosphere, simulated by the novel CORSIKA 8 framework. The simulated spectra of secondaries, such as pions, kaons, baryons and muons, are compared with the cascade equations solvers MCEq in air shower mode, and full 3D air shower Monte Carlo simulations using the legacy CORSIKA 7. A novel capability of CORSIKA 8 is the simulation of cascades in media other than air, widening the scope of potential applications. We demonstrate this by simulating cosmic ray showers in the Mars atmosphere, as well as simulating a shower traversing from air into water. The CORSIKA 8 framework demonstrates good accuracy and robustness in comparison with previous results, in particular in those relevant for the production of muons in air showers. Furthermore, the impact of forward ρ^0 production on air showers is studied and illustrated.

37th International Cosmic Ray Conference (ICRC 2021)
July 12th – 23rd, 2021
Online – Berlin, Germany

*Presenter

1. Introduction

The capabilities of the CORSIKA 8 framework [1] for particle cascade simulations are used to study the level of accuracy of hadron cascade simulations by comparing different approaches. Hadron cascades are in the core of cosmic ray air showers and are, thus, of high importance for the formation of the subsequent electromagnetic cascade as well as the muon and neutrino production in air showers [8]. For this work we are using the version *icrc-2021-b* of CORSIKA 8, which includes Sibyll2.3d [2] and QGSJetII.4 [3], as well as tracking in magnetic fields. Furthermore, we will exploit and illustrate the capabilities with non-air and exo showers, consistently developing in various materials other than the Earth atmosphere.

Some of the current capabilities of CORSIKA 8 are shown, and the resulting hadron cascades are compared in detail to other results and simulation programs. A general understanding of hadron cascades in the most systematic way possible will be one of the cornerstones to better understand uncertainties in air shower simulations and to further improve the quality of simulations. The work presented here makes use of the high degree of modularity allowed and encouraged inside CORSIKA 8, which can be easily extended as needed to tackle a wide range of problems.

2. High-energy models

The high-energy interaction models Sibyll2.3d and QGSJetII.4 are simulated with CORSIKA 8 (release: *icrc-2021-b*), CORSIKA 7 [4] (v7.7410) and MCEq [5] (v1.2.1, including Sibyll2.3c). The Linsley approximation of the US-standard atmosphere is used to approximate the Earth atmosphere. Here, we focus on vertical, proton-induced showers at $E_0 = 10^{18}$ eV without thinning. Only the

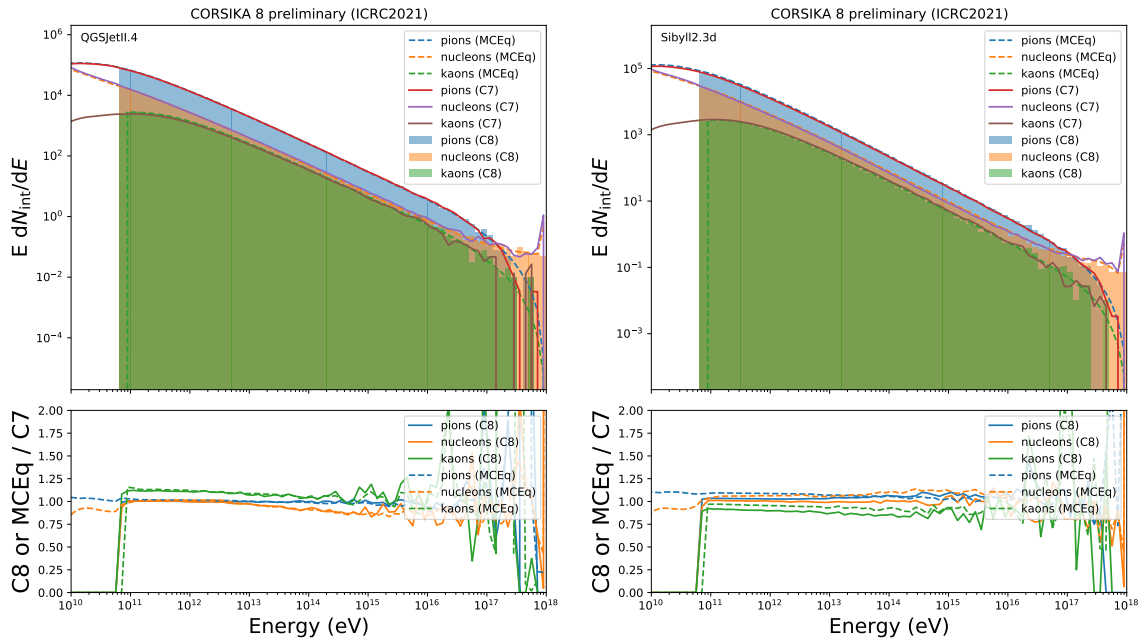


Figure 1: Total number of interaction as a function of projectile lab energy for various projectiles in the cascade for QGSJetII.4 (left) and Sibyll2.3d (right). Particles with kinetic energies above 63.1 GeV are shown.

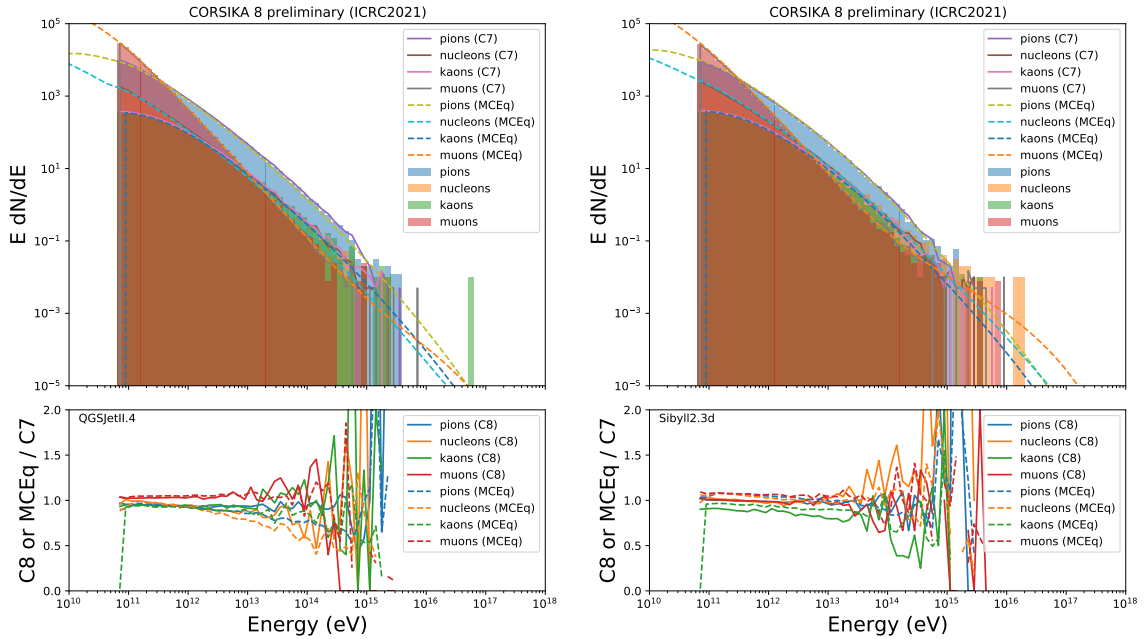


Figure 2: Secondary particle spectra at observation level (1400 m a.s.l) for QGSJetII.4 (left) and Sibyll2.3d (right).

high-energy models are used (for $E_{\text{lab}} > 63.1$ GeV), no low-energy model is used. Particles with energies below 63.1 GeV are removed. For each result 200 showers are simulated and averaged.

One of the most critical distribution to study is the overall total energy distribution of collisions in the entire cascade. Each collision is responsible for multi-particle production, thus, deviations in the number of collisions have large impact on the final structure of the air shower. In Figure 1 these distributions are shown and compared to the ones of CORSIKA 7 as a reference. For QGSJetII.4 the agreement between CORSIKA 8 and MCEq is virtually perfect, while with CORSIKA 7 better than $\approx 10\%$ with some energy-dependence. We note that for a model like QGSJetII.4 there is some freedom of interpretation in the interface to the model; we made an effort to synchronize our interface as much as possible with MCEq here.

For Sibyll2.3d the agreement of pions and nucleons with CORSIKA 7 is close to perfect, while there is a deficit of kaons on a level of $\approx 15\%$. Note, that the MCEq version used here contains Sibyll2.3c with known deviations in particle production.

If we study the secondary particle spectra at Malargüe ground level (1400 m above sea level corresponding to 875.5 g/cm^2) we find the results shown in Figure 2. The agreement is generally very good. Interestingly, the prediction for the muon energy spectrum comes out as the most robust prediction between all the investigated models. While for QGSJetII.4 the muon spectra ratios are completely energy independent, for Sibyll2.3d there is a very small energy dependence seen, which deserves further studies. Also there is a small but noticeable kaon deficit.

Moreover, the lateral arrival of secondary particles at the ground level was studied with CORSIKA 7 and CORSIKA 8. The results are shown in Figure 3 (left). There is an interesting systematic effect of a slightly wider shower footprint in CORSIKA 8 with respect to CORSIKA 7 visible. While this is a relatively small effect, it may well be important since detectors are often at far core distance and may notice this. However, the origin of this effect is not yet understood or

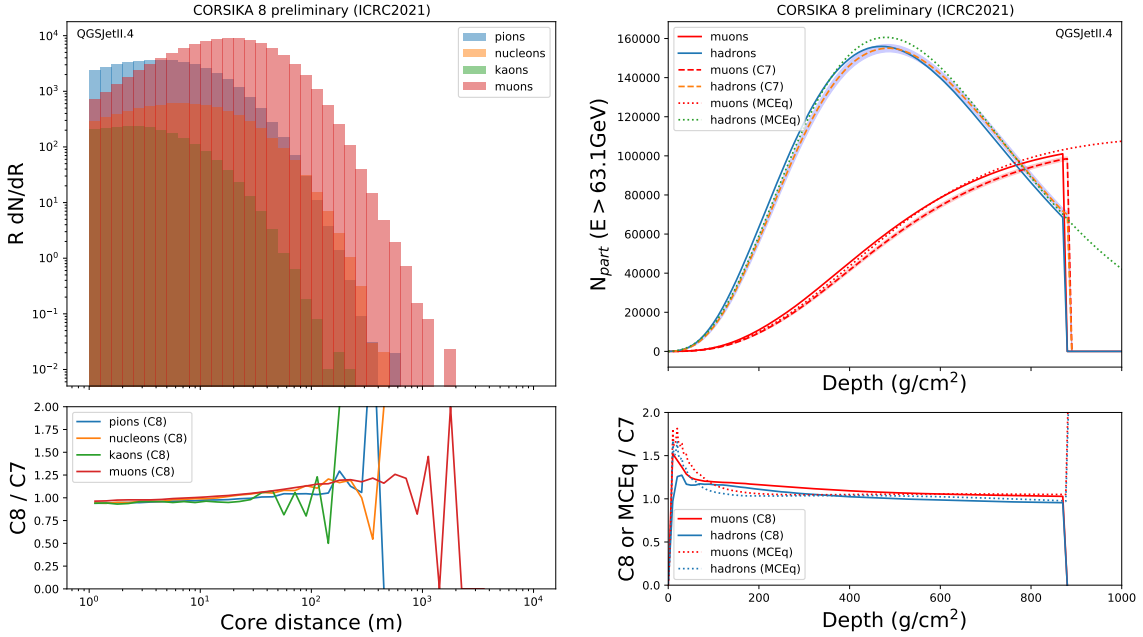


Figure 3: Left panel: Lateral particle number distribution for QGSJetII.4 comparing CORSIKA 8 and CORSIKA 7. Right panel: Longitudinal particle number profile for QGSJetII.4 comparing CORSIKA 8 to CORSIKA 7 and MCEq. Particles with kinetic energies above 63.1 GeV are shown.

even fully studied – this will be further pursued by the CORSIKA 8 Collaboration.

Finally, in Figure 3 (right) we show the comparison of a longitudinal particle number profile for muons and hadrons, where the latter are the sum of π^\pm , $K_{L/S}^0$, K^\pm , n , p , Λ (and their anti-baryons). For CORSIKA 7 the uncertainty of the average profile is shown as a shaded band. The magnitude of this uncertainty depicts also an estimate of the uncertainty of the other profiles. The agreement is generally within statistical uncertainties, however, there are small systematic deviations visible consistent with the results shown above. CORSIKA 8 has a few more muons than CORSIKA 7. CORSIKA 8 indicates a general slightly slower shower development compared to MCEq and CORSIKA 8. MCEq has a slightly more narrow profile in general.

3. Investigating of $\rho^0 \leftrightarrow \pi^0$ conversion

The particular importance of forward ρ^0 production in pion-air collision was found earlier [9, 10]. Following the method presented in Ref. [12] we developed a novel method for ad-hoc conversion of $\rho^0 \leftrightarrow \pi^0$ in air showers. This was implemented inside the CORSIKA 8 framework and used to simulated the impact for various levels of conversion. The conversion factors are energy dependent and are limited to the interval $[-1, 1]$:

$$p(E) = \text{clamp} \left(p_0 + \frac{f_{19} - p_0}{\log \frac{E_{\text{th}}}{10^{19} \text{ eV}}} \max \left(0, \log \frac{E}{E_{\text{th}}} \right) \right) \quad (1)$$

where $\text{clamp}(x)$ is defined as $\text{clamp}(x) = \min(1, \max(-1, x))$. For $p(E) > 0$ we replace $\pi^0 \rightarrow \rho^0$ with probability $p(E)$. For negative values we replace $\rho^0 \rightarrow \pi^0$ with probability $-p(E)$.

This method is applied to Sibyll2.3d proton showers. The effect is illustrated in Figure 4. While the electromagnetic $dE/dX|_{\text{max}}$ is anti-correlated with f_{19} by a few percent, the muons at ground

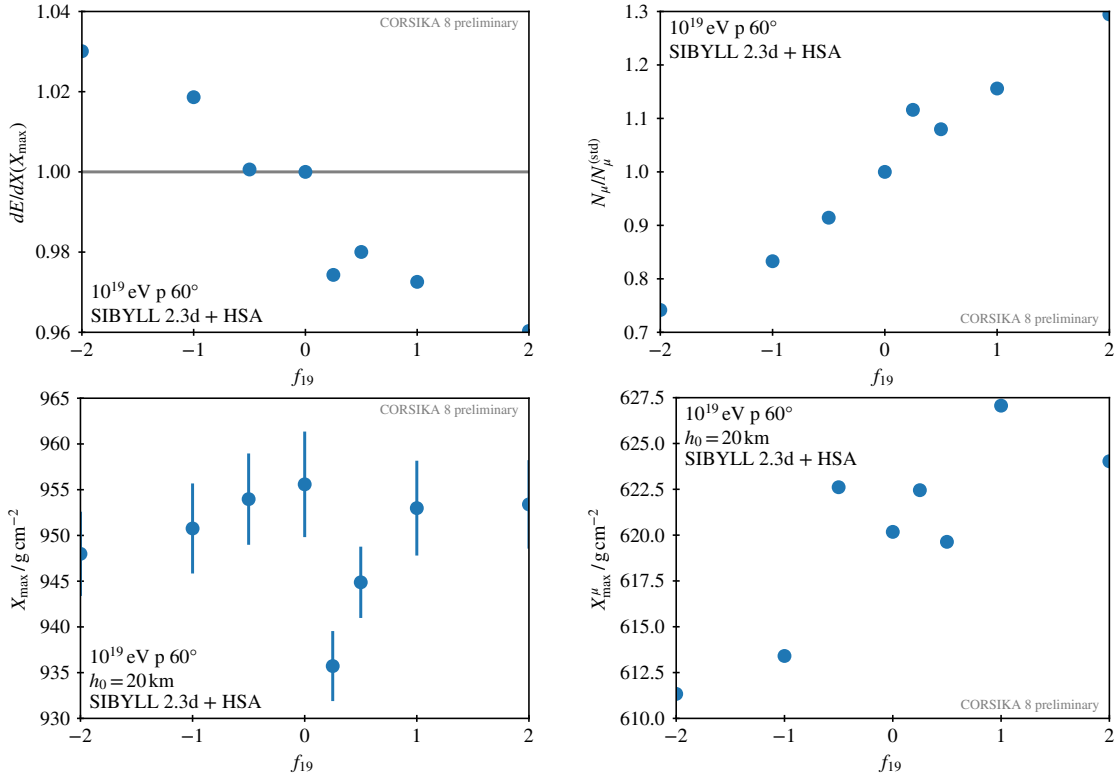


Figure 4: Overview of the results of converting $\rho^0 \leftrightarrow \pi^0$ in air showers. Top left is $dE/dX|_{\max}$ normalized to 1 at the reference point, top right is the muon number at ground, bottom left X_{\max} and bottom right X_{\max}^{μ} . Secondary particles with kinetic energies above 1 GeV are shown.

are correlated and can change by tens of percent. At the same time, the longitudinal development of showers is hardly affected, both, X_{\max} and also X_{\max}^{μ} are affected at most by a negligible degree.

For the work presented here the Hillas-splitting-algorithm (HSA) [14] as contained in AIRES [6] is used inside CORSIKA 8 for all kinetic lab energies below 63.1 GeV. Particles with kinetic energies below 1 GeV are removed. Furthermore, all produced photons (and also few electrons) from hadron collisions are used as input for CONEX [7] 1D longitudinal profile calculations to derive a full energy deposit profile including X_{\max} . For this purpose, CONEX is run inside CORSIKA 8 as another physics module. This provides robust estimates of dE/dX and, thus, X_{\max} .

4. Non-standard showers

The modularity and flexibility of CORSIKA 8 and its provided media-description facilities allow for the straightforward configuration of non-standard environments, thus, non-air or even exo-showers. Materials, geometries, magnetic fields, and in general: all properties of volumes, can be easily configured as needed by users.

4.1 Exo-showers on Mars

The integrated density column of the Mars atmosphere is just a few percent compared to Earth. Vertical showers see almost no material before they hit the ground. We implemented a two-layer

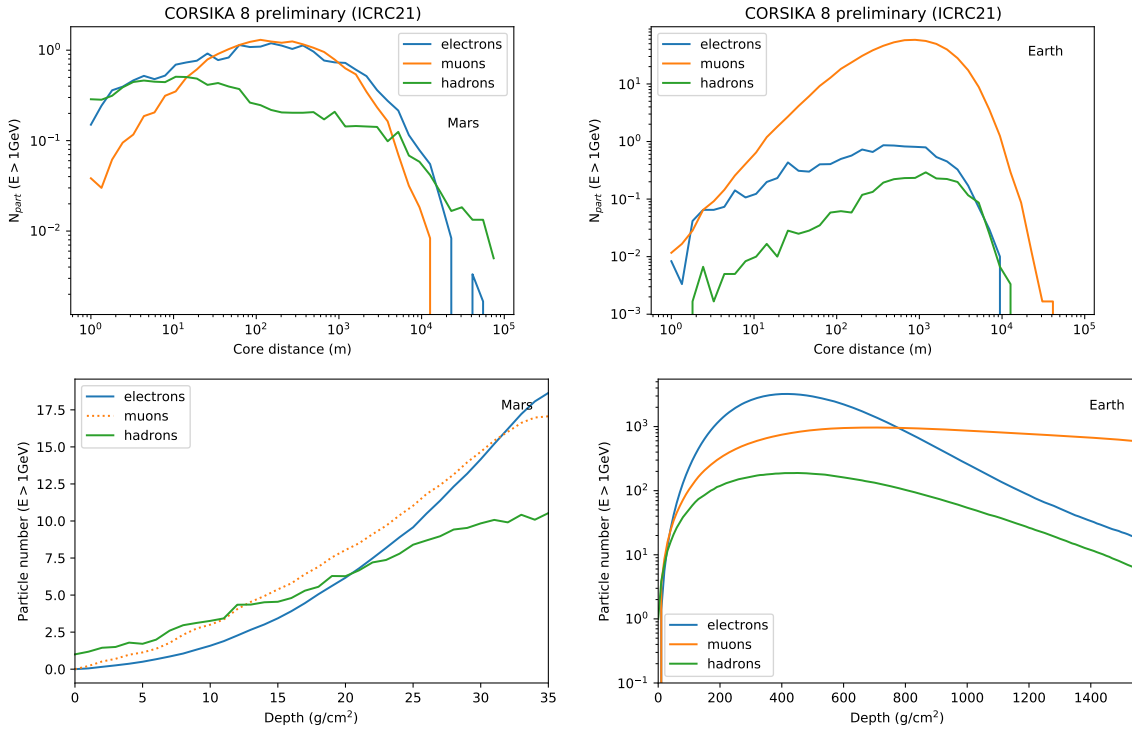


Figure 5: Summary of 100 TeV proton induced showers on Mars (left) and Earth (right) at 60° of zenith angle. On the top lateral particle number distributions on ground level are shown, while on the bottom this is shown for longitudinal profiles. Secondary particles with kinetic energy above 1 GeV are shown.

Mars atmosphere and simulated inclined ($\theta = 60^\circ$) proton showers on Earth and on Mars with a <1 GeV particle cutoff. The low energy model is UrQMD with a transition at $E_{kin,lab} = 63.1$ GeV to the high energy model Sibyll2.3d. Furthermore, E.m. interactions are fully simulated with PROPOSAL. Earth has a magnetic field strength of $50 \mu T$ and a standard Linsley atmosphere, while Mars has no magnetic field and a two layer density model provided by NASA [11]. Due to a current technical limitation of UrQMD in CORSIKA 8 the atmosphere composition of Mars is kept as 78% nitrogen and 22% oxygen instead of almost pure CO₂. In the future this is not going to be necessary – but it will hardly affect the results shown here. The results in lateral and longitudinal direction are shown in Figure 5. Shown are the averages over 600 showers. Indeed, the showers on Mars are seen in very early stages of their development. It will be an interesting further study to include the Mars soil into the simulations to determine a full picture of the effect of cosmic radiation on the surface of Mars.

4.2 Showers with a transition from air to water

When the observation level of CORSIKA 8 is moved to (negative) 3 km below sea level, the material between sea level and the observation level can be configured to be constant-density water with the correct, known, ionization energy loss parameters. Showers will first normally develop in air until the transition surface between air and water, and then consistently enter into water and continue their development towards the observation level. Of course, any backscatter from the dense medium into air is absolutely possible, too. The density model is shown in Figure 6 (left).

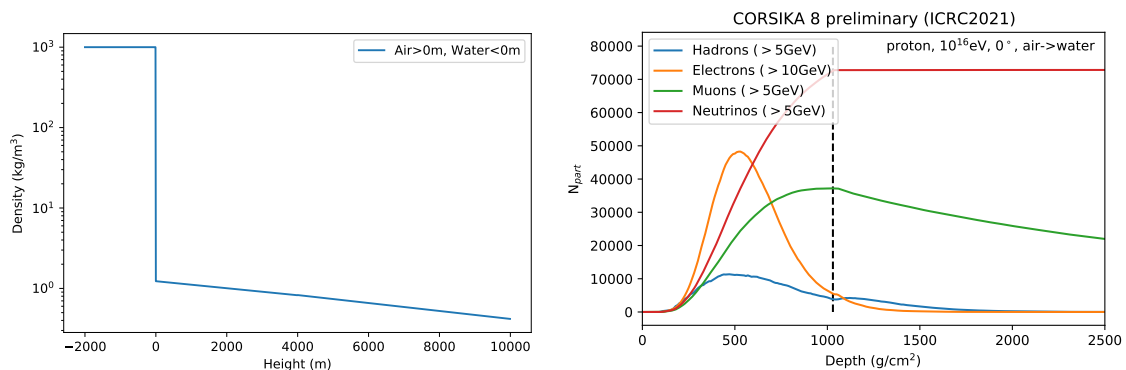


Figure 6: Left panel: Density model with a Linsley US std. atmosphere above sea level and water below sea level. Right panel: Longitudinal profile with a transition from air to water. The transition depth is shown as a dashed line. Note that the shown 1500 g/cm² of water depth just correspond to about 15 m of water column, while the simulation continues down to -3 km.

Here we use UrQMD for energies below 63.1 GeV and Sibyll2.3 above this. E.m. interactions are handled with PROPOSAL. Particles with energies below 5 GeV are removed; electrons and photons already at 10 GeV. Note, that currently PROPOSAL does not yet include density-dependent effects like LPM, but this will change in the future and will further improve such simulations.

In the resulting longitudinal particle number profile also neutrinos are included here, see Figure 6 (right), to illustrate the propagation through dense media. While the e.m. cascade is almost instantly absorbed in water, and muons start to be attenuated, the neutrinos are just continuing their trajectories to the observation level. It is interesting to note, that when the hadron core hits the dense media a very brief period of enhanced shower activity occurs – in distance this is just a few meters. While the properties in terms of ionization of water and air are just slightly different (e.g. critical energy in air is 88 MeV and in water 78 MeV) the main difference is the density and thus the energy loss per meter being a factor of ≈ 1000 higher in water. In combination, this leads to very efficient energy transport in water towards low energy particles (and below the cutoff energy of the simulation). In the longitudinal profiles this is evident since the regeneration of muons and also neutrinos in water above the energy cutoff is quite small. One can also imagine the conversion from depth to geometric distance to be very important. The decay of particles happens on geometric distance scale which is a factor of 1000 compressed in water compared to air, strongly suppressing the generation of new particles via decays per unit of depth.

5. Summary

CORSIKA 8 is becoming a highly versatile, fundamentally modular and powerful tool to perform particle cascade simulations. Sufficient completeness in term of provided models and robustness already allow for specific limited studies, many of which could not be done (easily) with other existing tools and programs. It was just started to perform real validation studies with CORSIKA 8, while in parallel more-and-more features and physics models are included.

In this work we have focused on a detailed comparison of air showers at high energies between different models and simulation programs. Preliminary results indicate agreement (mostly much) better than 10%, with a few points worth further investigations. For example kaon spectra are

a bit less consistently simulated, also there seem to be some small energy-dependent deviations. An indeed interesting result is that the LDF at sea level is slightly but systematically wider in CORSIKA 8 than in CORSIKA 7. Finally, longitudinal profiles simulated with CORSIKA 7 appear to be slightly slower in their development than, both, CORSIKA 8 and MCEq. This is even a bit more pronounced in MCEq than in CORSIKA 8.

In conclusion, CORSIKA 8 is shown to be already a partially powerful and robust tool for various novel and specific air shower physics studies. However, the framework is not yet ready for mass applications, further fundamental work is ongoing towards this direction. The project is open for collaborators and early users for testing, improvements, feedback and contributions [15].

References

- [1] R. Engel et al.. *Comput. Softw. Big Sci.* **3** (2019) 2. doi:10.1007/s41781-018-0013-0. arXiv:1808.08226 [astro-ph.IM].
- [2] F. Riehn, R. Engel, A. Fedynitch, T. K. Gaisser and T. Stanev. *Phys. Rev. D* **102** (2020) 063002. doi:10.1103/PhysRevD.102.063002. arXiv:1912.03300 [hep-ph].
- [3] S. Ostapchenko. *Phys. Rev. D* **83** (2011) 014018. doi:10.1103/PhysRevD.83.014018. arXiv:1010.1869 [hep-ph].
- [4] D. Heck, J. Knapp, J. N. Capdevielle, G. Schatz and T. Thouw. *FZKA-6019*.
- [5] A. Fedynitch, H. Dembinski, R. Engel, T. K. Gaisser, F. Riehn and T. Stanev. *PoS ICRC2017* (2018) 1019. doi:10.22323/1.301.1019.
- [6] S. J. Sciutto. doi:10.13140/RG.2.2.12566.40002. arXiv:astro-ph/9911331 [astro-ph].
- [7] T. Bergmann, et al. *Astropart. Phys.* **26** (2007) 420. doi:10.1016/j.astropartphys.2006.08.005. arXiv:astro-ph/0606564 [astro-ph].
- [8] A. Fedynitch, M. Huber. *Proceedings of 37th International Cosmic Ray Conference, PoS ICRC2021*.
- [9] H. J. Drescher. *Phys. Rev. D* **77** (2008) 056003. doi:10.1103/PhysRevD.77.056003. arXiv:0712.1517 [hep-ph].
- [10] S. Ostapchenko. *EPJ Web Conf.* **52** (2013) 02001. doi:10.1051/epjconf/20125202001.
- [11] <https://www.grc.nasa.gov/www/k-12/airplane/atmosmrm.html>.
- [12] R. Ulrich, R. Engel and M. Unger. *Phys. Rev. D* **83** (2011) 054026. doi:10.1103/PhysRevD.83.054026. arXiv:1010.4310 [hep-ph].
- [13] R. Ulrich, C. Baus and R. Engel. *EPJ Web Conf.* **99** (2015) 11001. doi:10.1051/epjconf/20159911001.
- [14] A. M. Hillas. *Nucl. Phys. B Proc. Suppl.* **52** (1997) 29. doi:10.1016/S0920-5632(96)00847-X.
- [15] gitlab.ikp.kit.edu/AirShowerPhysics/corsika.

GPU accelerated optical light propagation in CORSIKA 8

Dominik Baack^{a,*} and Wolfgang Rhode^a on behalf of the CORSIKA 8 Collaboration
(a complete list of authors can be found at the end of the proceedings)

^a*TU Dortmund,*

Otto-Hahn-Strasse 4a, Dortmund, Germany

E-mail: dominik.baack@tu-dortmund.de, wolfgang.rhode@tu-dortmund.de

Optical photons, created from fluorescence or Cherenkov emission in atmospheric cascades induced through high energetic cosmic rays are of major interest for several experiments. Experiments like CTA require a significant amount of computing time and funds for the simulation with CORSIKA 7.

Since individual photons don't interact they can be simulated without any order. The traditional sequential approach is simple but leads to reduced utilization of modern hardware infrastructure. The calculations done on each photon have low complexity, compared to the other aspects of the simulation. This, as well as the fact that, besides information about the photon itself, nearly no additional data is needed, favors a data-parallel approach in which several photons are propagated concurrently. The new CORSIKA 8 framework enables the implementation and verification of these methods.

With the use of dedicated high parallel acceleration hardware like GPUs the possible benefits with this data-parallel approach are even higher.

*** 37th International Cosmic Ray Conference (ICRC2021), ***

*** 12-23 July 2021 ***

*** Berlin, Germany - Online ***

*Presenter

1. Optical light in atmospheric cascades

For the observation of high-energy cosmic rays, direct observation by satellite-based experiments is currently not possible, due to their comparably low rate. Large-scale Earth-based observations, on the other hand, are hampered by the complex cascading interactions within the atmosphere. To address this problem high-quality simulations of the entire cascade are required to gain meaningful insight from the observed parameters. Large simulation samples are therefore of great importance, but in many cases can only be achieved, if at all, with massive computational and thus equally high costs. Several physical properties of the shower can be used as the observable/measurable parameters. One frequently used feature is the well detectable emission of light in the optical wavelength range in the form of Cherenkov radiation and fluorescent light within the forming cascade. With over 80% the first is one of the most run-time intensive parts in the simulation chain, due to their very large number of individual photons.

In this work, the completely redeveloped C++17 simulation framework CORSIKA 8 [1] is used. This is the successor of the widely used Fortran simulation software CORSIKA 7 [2], which is difficult to modernize due to its age and architecture. Due to the steadily-advancing evolution of computer hardware from former single CPU cores to today's highly parallel heterogeneous systems, the previous linear and iterative approach [3] used in CORSIKA 7 is no longer optimal for today's hardware. A different approach to the GPU implementation described in the following chapters is the optimization of the previous method using vectorization [4].

Based on previous work of the author [5] and to leverage the extensive development of deep-learning hardware, like the high processing power of modern graphics processors, the development was focused on NVIDIA's CUDA [6] architecture. This should facilitate better and more simulations for future experiments.

2. Accelerated Architecture

The complete simulation chain for the generation and propagation of Cherenkov and fluorescence light emission described here is currently a Python program, utilizing PyCuda [7], which is separated from the main CORSIKA framework to allow an easier evaluation, cross-checking, and rapid changes of the developed GPU kernels. The CORSIKA output of individual particle traces is directly transferred to Python and then the GPU to be processed further.

For the overall GPU side processing of particle tracks several modules could be reduced between the two different physical phenomena. On difference beside the generation itself is the "Filter Stage". Due to the fact that fluorescence emission is isotropic and not beamed like Cherenkov radiation, there is no early removal of particles applicable.

To utilize the full computational power of graphics co-processors, several special conditions must be met. The most important of these is the data- and time-parallel execution of all operations. This prohibits calculation on individual or a small number of traces, without massive performance degradation. Thus, to ensure that there is always enough data present to keep all cores active, there must be multiple parallel instances of CORSIKA present. The execution pattern for the first two operations is data-parallel at the particle track level. The subsequent operations are parallelized at the photon level.

2.1 Track Input

In the currently utilized version of the input handler, the curvature of the particle traces due to external factors, such as the geomagnetic field, is handled by the CORSIKA routines. To abstract from this, the common simplification of the particle tracks as line segments with a length corresponding to the acceptable error rate takes place. To reduce the workload on the CPU side and avoid additional branching, all traces are passed directly to the GPU, regardless of whether they can produce optical light emission.

On the GPU side, a first pass of the data applies some rough cuts in energy and charge to remove data that could create floating-point problems later on. In addition, the data is moved and restructured to allow for faster processing later on.

2.2 Filter Stage

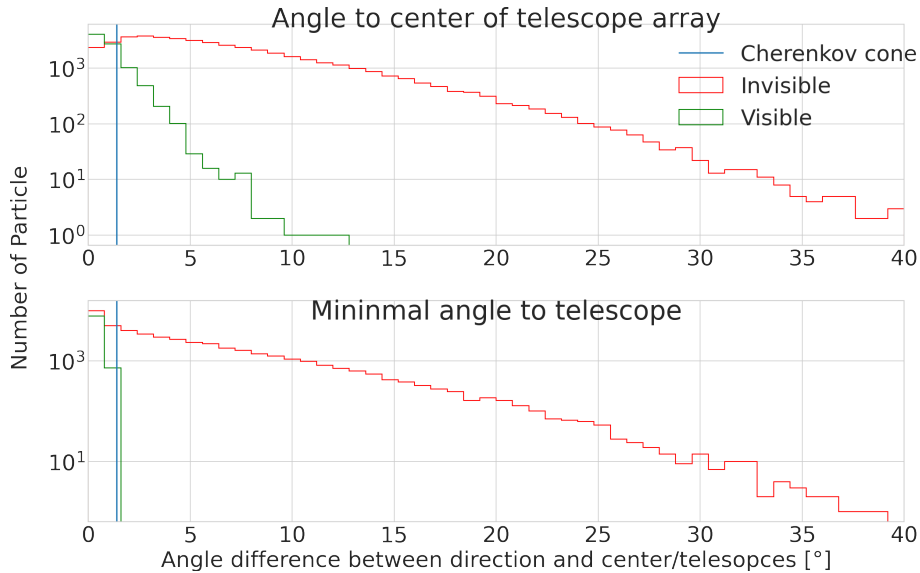


Figure 1: Displayed are two features of different computing complexity that allow the separating of tracks that, with a high probability, will not contribute to the observable Cherenkov photons. As basis for this analysis the preliminary locations and telescope sizes of the CTA North side were used.

Even though graphics co-processors are massively more powerful than CPUs, the efficient avoidance of unnecessary computations by suitable methods allows a significant reduction of runtime, despite the resulting overhead. The simplest applicable method for reducing the number of track segments passing the initial "Input Stage" (2.1) consists mainly of a single geometric cut. Depending on the energy of the shower and the expected amount of photons, one can choose, between a simple method that uses the angle between the flight direction and the vector to the center of the experiment, and a more computationally intensive method that uses the minimum angle between the flight direction and all experiment locations. In Figure 1 the preliminary positions of CTA North [8] were used for this purpose to demonstrate the worst-case effectiveness of the methods. For this worst-case study, a series of vertically incident was simulated using 1 TeV Gamma as initial particle. With cuts made at 12° or 5° , a reduction of $\sim 14\%$ resp. $\sim 32\%$ was achieved.

2.3 Photon Generation

The generation of photons can be divided into three parts:

- Calculating the number of photons
- Sampling of the emission point
- Calculating the direction of emission

Due to the different physical properties behind the emissions, two different kernels were developed.

2.3.1 Cherenkov Light

Calculating the number of photons emitted by each track is done with the Frank-Tamm formula, which leads to the following formalism:

$$N_{\text{cher}} = 2\pi\alpha z^2 L \frac{\lambda_1 - \lambda_2}{\lambda_1 \cdot \lambda_2} \cdot (1 - (n\beta)^{-2}), \quad (1)$$

with charge z , wavelength λ , refractive index n and track length L . Because of its small influence of much less than 1 ‰ on the amount of photons created, atmospheric light dispersion is neglected by averaging the wavelength-dependent refractive index over the interval of interest. If required dispersion can be added in the future with the accompanying loss in performance. To reduce the additional workload imposed by the artificial splitting of particle tracks used by the classic midpoint formalism, in which all photons are emitted from the track center, the default track length given by CORSIKA is maintained. To avoid imprecise handling and increase the simulation accuracy, the photon origin is sampled by an exponential distribution fitted to the local refractive index profile.

The photon emission direction is first generated in the vertical direction:

$$(\cos(\varphi_{\text{rand}}) \sin(\theta_c), \sin(\varphi_{\text{rand}}) \sin(\theta_c), -\cos(\theta_c))^T,$$

then rotated into the correct particle reference frame.

2.3.2 Fluorescence Light

Fluorescence emission can be calculated similarly to Cherenkov light in the previous section but with a light yield given by Kakimoto et al. [9]. One possible optimization is that not all photons have to be generated, but only those that point spatially in the direction of the experiment. This is done by reducing the solid angle to a small area and then sampling the random numbers from it.

2.4 Photon Propagation

A correct photon propagation through the atmosphere would involve a computing-intensive numerical integration along the path with changing refractive index. This scaled up for several million photons per shower would result in a slow down of several orders of magnitude even with GPUs. On the other hand, rectilinear propagation is very fast, but leads to errors that increase sharply with the zenith angle.

The combined approach allows a significant reduction of the physical inaccuracies without affecting the propagation time too much. For this purpose, an interpolation table is created before

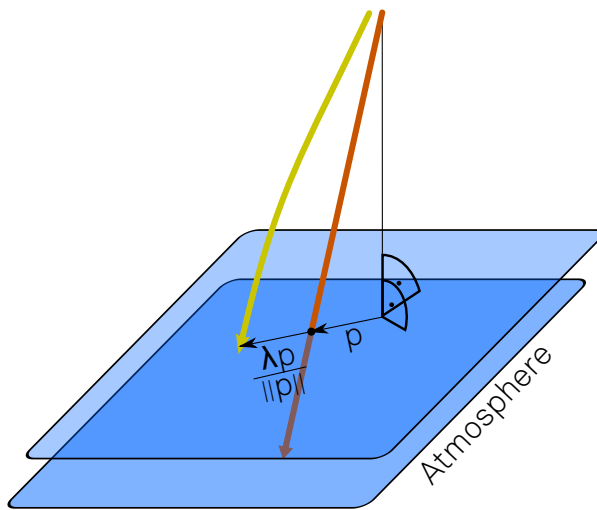


Figure 2: Displayed is the schematic structure of the planar Atmosphere with correction factor λ .

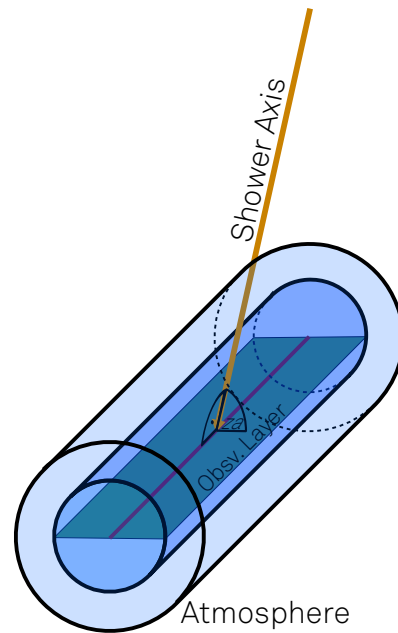


Figure 3: Shown is the schematic structure of the cylindrical atmospheric. Here the red main axis is a tangent to the earth's surface and orthogonal to the shower axis (orange).

the simulation, which contains a multiplicative correction factor. This can then be applied to the impact point of the photon to shift it accordingly. In addition, these corrections are also made with the time of arrival and the angle of impact. This procedure is already used in a similar form in CORSIKA 7.

The atmosphere description used as example here is the so-called "US standard atmosphere" [10] model. Depending on the required precision or run-time different simplification can be made. The simplest and fastest model is the assumption of planar atmosphere, i.e. without Earth curvature. This assumption allows to exploit symmetries that significantly reduce the required complexity to 2D and so the size of the tables. This table is as example displayed in Figure 4. It displays the scaling factor λ , which describes the shift along the normalized project vector on the ground plane as seen in Figure 2.

The use of specialized GPU hardware, the so-called texture unit, allows an extremely efficient interpolation between the individual values of the 2D table. This is done in parallel to the other computations, so that the method has almost the same runtime properties as the strictly linear propagation.

Even for this model the error drastically increases at very high zenith angles because the simplification as a plane atmosphere shows a strong deviation from the real-world behavior. However, a table generated for this purpose is considerably more extensive and, with 4 dimensions, no longer be interpretable in hardware. Further work shows promising results by removing one dimension and interpolating the atmosphere as a long cylinder (Figure 3) instead.

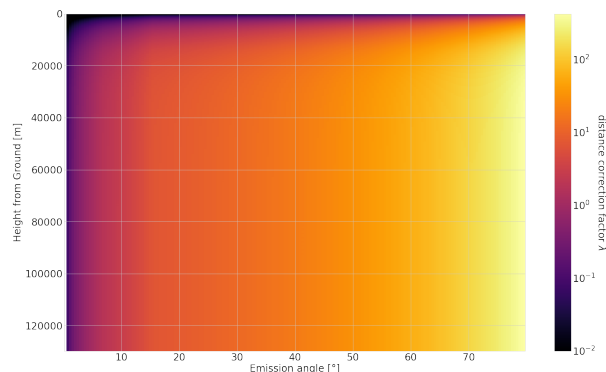


Figure 4: Correction factor for the straight line propagation based on a simplified planar atmosphere model.

2.4.1 Output

After propagation of the individual photons there is a last reduction step to reduce transfer time between GPU and CPU. This step removes all photons not hitting predefined areas. Those are usual telescope positions, but can be extended to encompass the whole shower. One sample is shown in Figure 5 displaying the unfiltered cascade, light emission on ground and the preliminary CTA Position projected on a 2D layer.

3. Summary and Outlook

The implementation of Cherenkov light for highly parallel hardware like GPUs shows promising results in terms of overall performance and flexibility. The statistical comparison between the classic photon generation and the GPU solution still needs to be extended and additional systematic studies with Cherenkov telescopes need to be performed.

After testing is complete the kernels will be moved out of the Python applications to the C++ framework to allow easier use and faster interconnect between CPU and GPU code.

Acknowledgments

Part of this work is supported by Deutsche Forschungsgemeinschaft (DFG) within the Collaborative Research Center SFB 876 4 "Providing Information by Resource-Constrained Analysis", project C3.

References

- [1] M. Reininghaus and R. Ulrich, *CORSIKA 8 – Towards a modern framework for the simulation of extensive air showers*, *EPJ Web Conf.* **210** (2019) 02011 [1902.02822].
- [2] D. Heck, J. Knapp, J.N. Capdevielle, G. Schatz and T. Thouw, *CORSIKA: A Monte Carlo code to simulate extensive air showers*, Tech. Rep. FZKA-6019, Forschungszentrum Karlsruhe (1998), DOI.

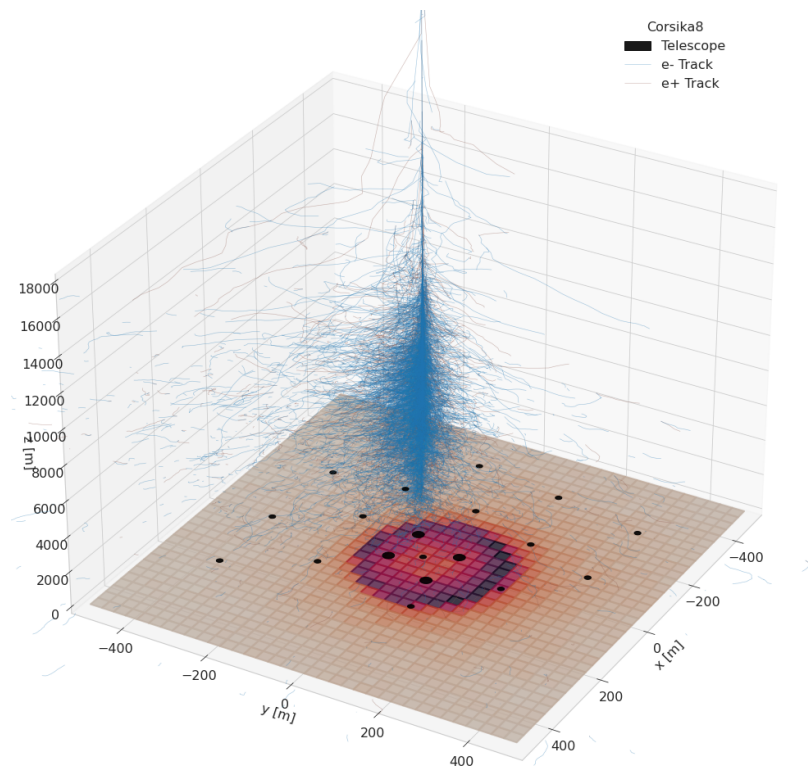


Figure 5: Displayed is a 1 TeV shower with its cherenkov light distribution on ground level.

- [3] K. Bernlöhner, *Impact of atmospheric parameters on the atmospheric cherenkov technique*, *Astroparticle Physics* **12** (2000) 255.
- [4] M. Carrère, *A c++ cherenkov photons simulation in corsika 8*, EPJ Web Conf., in press.
- [5] D. Baack and W. Rhode, *Gpu based photon propagation for corsika 8*, in *Journal of Physics: Conference Series*, vol. 1690, p. 012073, IOP Publishing, 2020.
- [6] I. Buck, *Gpu computing with nvidia cuda*, in *ACM SIGGRAPH 2007 courses*, pp. 6–es (2007).
- [7] A. Klöckner, N. Pinto, Y. Lee, B. Catanzaro, P. Ivanov and A. Fasih, *Pycuda and pyopencl: A scripting-based approach to gpu run-time code generation*, *Parallel Computing* **38** (2012) 157.
- [8] K. Bernlöhner, A. Barnacka, Y. Becherini, O.B. Bigas, E. Carmona, P. Colin et al., *Monte carlo design studies for the cherenkov telescope array*, *Astroparticle Physics* **43** (2013) 171.
- [9] F. Kakimoto, E. Loh, M. Nagano, H. Okuno, M. Teshima and S. Ueno, *A measurement of the air fluorescence yield*, *Nuclear Instruments and Methods in Physics Research Section A: Accelerators, Spectrometers, Detectors and Associated Equipment* **372** (1996) 527.

- [10] N. Sissenwine, M. Dubin and H. Wexler, *The us standard atmosphere, 1962*, *Journal of Geophysical Research* **67** (1962) 3627.